Nat. Hazards Earth Syst. Sci., 11, 2859–2879, 2011
www.nat-hazards-earth-syst-sci.net/11/2859/2011/
doi:10.5194/nhess-11-2859-2011

Natural Hazards and Earth System Sciences

A multidisciplinary analysis for traces of the last state of earthquake generation in preseismic electromagnetic emissions

S. M. Potirakis[1], **G. Minadakis**[2], **C. Nomicos**[3], **and K. Eftaxias**[4]

[1]Department of Electronics, Technological Education Institute (TEI) of Piraeus, 250 Thivon & P. Ralli, 12244, Aigaleo, Athens, Greece
[2]Department of Electronic and Computer Engineering, Brunel University Uxbridge, Middlesex, UB8 3PH, UK
[3]Department of Electronics, Technological Education Institute (TEI) of Athens, Ag. Spyridonos, 12210, Aigaleo, Athens, Greece
[4]Department of Physics, Section of Solid State Physics, University of Athens, Panepistimiopolis, 15784, Zografos, Athens, Greece

Received: 27 June 2011 – Revised: 5 September 2011 – Accepted: 12 September 2011 – Published: 26 October 2011

Abstract. Many questions about earthquake (EQ) generation remain standing. Fracture induced electromagnetic (EM) fields allow real-time monitoring of damage evolution in materials during mechanical loading. An improved understanding of the EM precursors has direct implications for the study of EQ generation processes. An important challenge in this direction is to identify an observed anomaly in a recorded EM time series as a pre-seismic one and correspond this to a distinct stage of EQ generation. In previous papers (Kapiris et al., 2004; Contoyiannis et al., 2005; Papadimitriou et al., 2008), we have shown that the last kHz part of the emerged precursory EM activity is rooted in the fracture of the backbone of asperities distributed along the activated fault, sustaining the system. The crucial character of this suggestion requires further support. In this work we focus on this effort. Tools of information theory (Fisher Information) and concepts of entropy (Shannon and Tsallis entropies) are employed. The analysis indicates that the launch of the EM precursor is combined with the appearance of a significantly higher level of organization, which is an imprint of a corresponding higher level of organization of the local seismicity preceding the EQ occurrence. We argue that the temporal evolution of the detected EM precursor is in harmony with the Intermittent Criticality approach of fracture by means of energy release, correlation length, Hurst exponent and a power-law exponent obtained from frequency-size distributions of seismic/electromagnetic avalanche events. The candidate precursory EM activity is also consistent with other precursors from other disciplines. Thus, accumulated evidence, including laboratory experiments, strengthen the consideration that the emergence of the kHz EM precursor is sourced in the fracture of asperities indicating that EQ occurrence is expected.

Correspondence to: K. Eftaxias
(ceftax@phys.uoa.gr)

1 Introduction

Earthquakes (EQs) are large-scale fracture phenomena in the Earth's heterogeneous crust. Despite the large amount of experimental data and the considerable effort that has been undertaken by the material scientists, many questions about fracture processes, and especially the EQ generation processes, remain standing .

It is reasonable to expect that EQs' preparatory process has various facets which may be observed before the final catastrophe. Therefore, the science of EQ prediction should be, from the start, multi-disciplinary. Fracture- induced fields allow a real-time monitoring of damage evolution in materials during mechanical loading. Electromagnetic (EM) emissions in a wide frequency spectrum ranging from kHz to MHz are produced by the cracks' opening, which can be considered as the so-called precursors of general fracture (Papadimitriou et al., 2008; and references therein). These precursors are detectable both at a laboratory (Bahat et al., 2005; Rabinovitch et al., 2001) and a geophysical scale (Gokhberg et al., 1995; Hayakawa and Molchanov, 2002; Uyeda et al., 2009).

Our main observational tool is the monitoring of the fractures which occur in the focal area before the final breakup by recording their kHz-MHz EM emissions. Recent results indicate that these pre-seismic EM time-series contain

information characteristic of an ensuing seismic event (Papadimitriou et al., 2008; Kapiris et al., 2004; Contoyiannis et al., 2005; Karamanos et al., 2006; Eftaxias, 2009). Being non-destructive, monitoring techniques based on these fracture-induced fields are a basis for a fundamental understanding of fracture mechanism and for developing consecutive models of rock/focal area behaviour. An improved understanding of the EM precursors, especially their physical basis, has direct implications for the study of EQ generation processes and EQ prediction research.

An important challenge in this field of research is to identify an emerged anomaly in a recorded EM time series as a pre-seismic one and correspond this to an individual stage of EQ preparation process. Herein, we focus on this direction.

An anomaly is defined as a deviation from normal (background) behaviour. In order to develop a quantitative identification of EM precursors, complementary tools of information theory and concepts of entropy are employed here to identify changes in statistical patterns.

One of the most important contributions of Information Theory is the establishment of a recipe for ascertaining in precise and unambiguous terms the amount of information, i.e. the information measure that an observer possesses concerning a given phenomenon when only a probability distribution is known. Actually, Shannon entropy (Shannon, 1948) provides a measure of lack of information, which is why its opposite (usually referred to as "negentropy", or "information", Brillouin, 1953; Frieden, 1990) is preferably used in communications theory, e.g. (Shanmugam, 2009). Increase of the information content (indicating order) corresponds to decrease of Shannon entropy and accordingly to an increase of Shannon information. Shannon information was considered as the major tool to describe information behaviour and complexity of physical systems. However, during the last years, a growing interest for information has arisen in theoretical physics; while no discussion of information measures can be regarded as complete without reference to that of Fisher (Fisher, 1925). Fisher information is a physically meaningful measure of disorder for many physical systems. Frieden (1990) characterized Fisher information as a versatile tool to describe the evolution laws of physical systems.

For systems exhibiting long-range correlations, memory, or fractal properties, nonextensive Tsallis' entropy, becomes an appropriate mathematical tool (Tsallis, 1988, 1998, 2009; Abe et al., 2007). A central property of the EQ preparation process is the occurrence of coherent large-scale collective behaviour with a very rich structure, resulting from repeated nonlinear interactions among the constituents of the system (Sornette, 2004; Rundle et al., 2003). Consequently, Tsallis entropy is also a physically meaningful tool for investigating the launch of a fracture-induced EM precursor.

From an information-theoretical point of view, Tsallis' entropy is, like Shannon's entropy, a "missing information" measure, while Fischer's information is a positive one (Frieden, 1990; Plastino et al., 1997; Martin et al., 1999). Therefore, Tsallis entropy (like Shannon entropy) "drops" have as a counterpart Fisher information "peaks", both indicating a more ordered state. In this sense, entropy and information are seen to be complementary quantities.

The application of both Fisher information and Shannon entropy to complex electroencephalogram (EEG) signals has been presented by Martin et al. (1999). One of the interesting results of their study is that Fisher information allowed the detection of non-stationary behaviour in situations where the Shannon entropy shows limited dynamics. On the other hand, Vignat and Bercher (2003) have shown that the analysis of complex, possibly non-stationary signals can be carried out in an information plane defined by both Shannon entropy and Fisher information.

A way to examine transient phenomena on a pre-seismic EM time series is to partition it into a sequence of distinct time windows. The aim is to discover a clear difference of dynamical characteristics as the catastrophic event is approaching. In this work, we concentrate on the candidate EM precursor associated with the Athens EQ. The Athens EQ, with a magnitude of 5.9, occurred on 7 September 1999. Clear EM anomalies at 3 and 10 kHz were simultaneously detected from a few days up to a few hours prior to this EQ (see Sect. 3).

Motivated by the above-mentioned concepts, we analyze the pre-seismic EM data successively in terms of Fisher Information, Shannon entropy and Tsallis entropy and compare their ability to identify an emerged EM anomaly. We argue that this analysis reliably distinguishes the candidate EM precursors from the noise: the launch of anomalies from the background state is combined with the appearance of a significantly higher level of organization. We state that if the detected EM anomaly is a result of the EQ preparation process, then its higher level of organization should be an imprint of a corresponding higher level of organization of the seismicity. Therefore, an important pursuit is to make a quantitative comparison between the temporal changes of the organization hidden in an emerged EM anomaly on one hand, and the changes of the organization of seismicity on the other hand, as the EQ is approaching. Our analysis confirms the aforementioned association. Finally, we examine whether the pre-seismic EM activity under study is compatible to the "Intermittent Criticality" (IC) (Sornette, 2004; Sornette and Sammis, 1995; Saleur et al., 1996a, b; Sammis et al., 1996; Heimpel, 1997) class of models. IC bridges the hypothesis of an underlying self-organized complexity to the occurrence of precursory phenomena. We argue that the present analysis further supports the consideration that the last kHz part of the emerged precursory EM activity is rooted in the last state of earthquake generation.

Since it is expected that the EQ's preparatory process has various facets which may be observed before the final catastrophe, a candidate precursory EM activity should be consistent with other precursors that are imposed by data from

other disciplines. Experimental evidence indicates that the above mentioned requirement is well-satisfied in the case under study.

This work is organized as follows. In Sect. 2 we provide concisely the necessary background knowledge on Shannon entropy, Fisher information, and Tsallis entropy. In Sect. 3 we proceed to the analysis of a well-documented precursory EM anomaly recorded prior to the Athens EQ, studying the evolution with time of Fisher information, Shannon entropy and Tsallis entropy. The main objective is to evaluate the effectiveness of the entropy/information metrics to examine transient phenomena. The results are combined with the results of the spectral fractal analysis for the same EM precursor. In Sect. 4, we study the associated seismicity in terms of the changes of its organization as the EQ is approaching first, and then in terms of Intermittent Criticality. Finally, in Sect. 5 we summarize and discuss our results.

2 Introduction to Shannon entropy, Fisher information, and Tsallis entropy

In this section we briefly provide the basic background knowledge and some useful formulae concerning the Shanon entropy, Fisher Information, and Tsallis entropy.

2.1 Shannon entropy

Suppose we have a set of n possible events whose probabilities of occurrence are $p_i, (i=1,2,...,n)$. The informational content of the specific normalized probability distribution is given by Shannon's information measure as (Shannon, 1948):

$$H_{\mathrm{sh}} = -K \sum_{i=1}^{n} p_i \log(p_i), \tag{1}$$

where K, is a positive constant (it merely amounts to a choice of a unit of measure, however it is usually set to 1). H_{sh} has been forwarded by Shannon as a measure of information, choice and uncertainty, and recognized as a form of entropy.

Increase of the information content (order) corresponds to decrease of Shannon entropy. Shannon entropy is considered a basic tool to describe the information behaviour and complexity of physical systems.

2.2 Fisher information

Fisher Information has been increasingly gaining the interest of scientists of different scientific fields over the last years. It was first introduced by Fisher (1925) as a representation of the amount of information in the results of experimental measurements of an unknown parameter of a stochastic system, or simply the amount of information that can be extracted from a set of measurements (or the "quality" of the measurements) (Mayer et al., 2006). Fisher information also provides the basis for a comprehensive alternative approach to the derivation of probability in physics and other sciences, and is a versatile tool to describe the evolution laws of physical systems (Frieden, 1990, 1998, 2004; Frieden and Gatenby, 2007; Frieden and Soffer, 2000). Moreover, it is a powerful tool to investigate complex and non-stationary signals (Martin et al., 1999; Telesca et al., 2011). It allows the accurate description of the behaviour of dynamic systems, and the characterization of the complex signals generated by these systems (Martin et al., 1999; Vignat and Bercher, 2003). The informative content of Fisher Information in detecting significant changes in the behaviour of nonlinear dynamical systems has been pointed out (Martin et al., 2001), rendering it an important quantity involved in many aspects of the theoretical and observational description of natural phenomena (Telesca et al., 2011). It has been used as a measure of the state of disorder of a system or phenomenon, behaving inversely to entropy, i.e. when order increases, entropy decreases, while Fisher Information increases (Mayer et al., 2006; Frieden, 1998). Furthermore, Fisher Information presents the so called "locality" property in contrast to the "globality" of entropy (or Shannon's information), referring to the sensitivity of Fisher Information to changes in the shape of the probability distribution corresponding to the measured variable, not presented by entropy (Mayer et al., 2006; Frieden, 2004; Fath and Cabezas, 2004). It has been used in studying several geophysical and environmental phenomena, revealing its ability in describing the complexity of a system, e.g. (Telesca et al., 2008; Balasco et al., 2008), and suggesting its use to reveal reliable precursors of critical events (Telesca et al., 2005a, b, 2009).

In order to provide some useful formulae, let's assume θ an unknown deterministic parameter of a process (system), x an observable stochastic variable $\left(x \in R^M, M \geq 1\right)$, from which θ can be determined, and $f_\theta(x)$ the probability density for x (depending also on θ). Trying to infer θ from measurements of x, one would end-up with an estimate $\hat{\theta}(x)$ of θ. The mean square error of the best possible estimator is low bounded by the inverse of a quantity called the Fisher Information Measure (FIM), named after Fisher who introduced it (Fisher, 1925), which is defined as (Frieden and Gatenby, 2007; Cramer, 1946; Plastino et al., 1997; Pennini et al., 2009):

$$I(\theta) = \int_{-\infty}^{\infty} dx \cdot f_\theta(x) \left[\frac{\partial \ln(f_\theta(x))}{\partial \theta} \right]^2. \tag{2}$$

As soon as the estimators are unbiased, the lower bound is the same indifferently to the parameter of the system one chooses to measure; the error has to be larger than or equal to the inverse of the Fisher information associated with the concomitant experiment (Frieden and Gatenby, 2007). The particular case of the translation families, i.e. distribution functions whose form does not change under θ displacements (i.e. shift invariant distribution functions), is of great importance

(Frieden and Gatenby, 2007; Frieden, 1998; Pennini et al., 1998). In that case FIM has a simple expression for the one-dimensional case. Then, FIM, I_x is defined (Martin et al., 1999, 2001; Frieden and Gatenby, 2007; Bercher, 2010) as:

$$I_x = \int_{-\infty}^{\infty} \left[\frac{\partial \ln(f(x))}{\partial x} \right]^2 f(x) dx = \int_{-\infty}^{\infty} \left(\frac{\partial f(x)}{\partial x} \right)^2 \frac{dx}{f(x)} \quad .(3)$$

In the case of a discrete measured variable $s_k = s(t_k)$, with $t_k = kT, k = 1, 2, ..., K$, and T being the sampling period, one can define a set of N disjoint but adjacent intervals (bins) covering the whole range of values between the minimum and maximum observed values of the time-series $\{s_k\}$, denoted as $\{x_n\}, n$=1, 2, ..., N. The corresponding probability for a sample of the time-series to belong to the n-th interval can be denoted as $p(x_n)$. Then, FIM of the Eq. (3), in its discrete form, can be expressed (Martin et al., 1999, 2001; Humeau et al., 2008; Cabezas and Karunanithi, 2008) as:

$$I_x = \sum_{n=1}^{N-1} \frac{\left[p(x_{n+1}) - p(x_n) \right]^2}{p(x_n)}. \quad (4)$$

The discrete probability distribution $p(x_n)$ corresponds to the specific values of the unknown underlying probability density function at the centre values of the intervals $\{x_n\}$, which are not necessarily of equal length. The probability density function is usually approximated by the histogram (Martin et al., 1999, 2001; Mercik et al., 1999; Lovallo et al., 2007), or by the kernel density estimator technique (Devroye, 1987; Janicki and Weron, 1994), employing different kernel functions like Gaussian kernel (Telesca et al., 2010, 2011; Raykar and Duraiswami, 2006), or Epanechnikov kernel (Telesca et al., 2009; Epanechnikov, 1969).

2.3 Tsallis entropy

In nature, long-range spatial interactions or long-range memory effects may give rise to very interesting behaviours. Among them, one of the most intriguing arises in systems that are non-extensive (non-additive). These systems share a very subtle property: they violate the Boltzmann-Gibbs (B-G) statistics, the bridge to the equilibrium thermodynamics. Inspired by multifractals concepts, Tsallis (Tsallis, 1988, 1998, 2009; Abe and Okamoto, 2001) proposed a generalization of the B-G statistical mechanics. He introduced an entropic expression, the Tsallis entropy, S_q, characterized by an index q which lead to a non-extensive statistics,

$$S_q = k \frac{1}{q-1} \left(1 - \sum_{i=1}^{w} p_i^q \right), \quad (5)$$

where p_i are the probabilities associated with the microscopic configurations, w is their total number, q is a real number, and k is Boltzmann's constant. The value of q is a measure of the non-extensivity of the system. Notice, $q = 1$ corresponds to the standard, extensive, B-G statistics.

The entropic index q characterizes the degree of non-extensivity reflected in the following pseudo-additivity rule:

$$S_q(A+B) = S_q(A) + S_q(B) + (q-1) S_q(A) S_q(B). \quad (6)$$

For subsystems that have special probability correlations, extensivity

$$S_{B-G}(A+B) = S_{B-G}(A) + S_{B-G}(B) \quad (7)$$

is not valid for S_{B-G}, but may Eq. (6) occur for S_q with a particular value of the index q. Such systems are referred to as non-extensive (Tsallis, 1998, 2009).

The cases $q > 1$ and $q < 1$, correspond to sub-extensivity, or super-extensivity, respectively. We may think of q as a bias-parameter: $q < 1$ privileges rare events, while $q > 1$ privileges prominent events (Zunino et al., 2008). We emphasize that the parameter q itself is not a measure of the complexity of the system but measures the degree of non-extensivity of the system. It is the time variations of the Tsallis entropy, S_q, for a given q that quantify the dynamic changes of the complexity of the system. Lower S_q values characterize signals with lower complexity.

3 Electromagnetic data analysis

A way to examine transient phenomena is to analyze the pre-seismic EM time series into a sequence of distinct time windows. The aim is to discover a clear difference of dynamical characteristic as the catastrophic event is approaching. Different metrics are applied on the detected pre-seismic EM emissions, each one having its own requirements.

A real acquired time-series is generally non-stationary. Fisher information is a powerful tool for the analysis of complex non-stationary signals (Martin et al., 1999; Telesca et al., 2010). On the other hand, entropy is computed in specific segments of the total time-series after they are proven to be stationary, e.g. (Papadimitriou et al., 2008; Kalimeri et al., 2008). In order to achieve comparable results, all employed metrics (Shannon entropy, Tsallis entropy, and Fisher information) are computed here versus time, by dividing the acquired time-series into time-windows of specific length with specific degree of overlapping and computing all metrics for each one of them. However, a stationarity check, using the technique described in (Karamanos et al., 2005), is performed beforehand. In case a time-window is found non-stationary, the calculation of the corresponding metrics for the specific window is omitted. Moreover, we analyzed the first difference of the raw data time series in order to remove the non-stationarities of the first order (Telesca et al., 2011).

In the following, we evaluate the effectiveness of the entropy/information metrics to examine transient phenomena by analyzing a pre-seismic EM time series into a sequence of distinct time windows and studying the resulting evolution with time of Fisher information, Shannon entropy, and Tsallis entropy.

As it was mentioned in the Introduction (Sect. 1), we concentrate on a well- documented, pre-seismic EM signal associated with the Athens EQ. The Athens EQ, with a magnitude of 5.9, occurred on 7 September 1999. Clear EM anomalies at 3 and 10 kHz were simultaneously detected from a few days up to a few hours prior to this EQ. In Fig. 1 we present the 10 kHz (East-West) EM time series from 4 July up to 11 September 1999. We mainly focus on this precursor for the following reasons: (i) it has a rather long duration, thus it provides sufficient data for a valuable statistical analysis; the data have been recorded with a sampling rate of 1 sample/s while the duration of the candidate EM precursor is more than six days. (ii) A multidisciplinary analysis in terms of fault modelling, laboratory experiments, scaling similarities of multiple fracturing of solid materials, fractal electrodynamics, criticality, complexity, universality, and mesomechanics seems to validate the association of the detected preseismic EM emission with the fracturing process in the focal area of the impending EQ (Papadimitriou et al., 2008; Bahat et al., 2005; Rabinovitch et al., 2001; Gokhberg et al., 1995; Hayakawa and Molchanov, 2002; Uyeda et al., 2009; Kapiris et al., 2004; Contoyiannis et al., 2005; Karamanos et al., 2006; Eftaxias et al., 2001, 2007, 2009; Kapiris et al., 2003, 2005). Figure 2 shows a zoom on the three epochs of the signal which are analysed in the following.

3.1 The Fisher information in its time-dependent fashion

We calculate the Fisher information associated with successive time-windows and study its evolution with time. We concentrate on the fundamental question whether distinguished alterations in associated Fisher information values emerge in the EM time series as Earth's crust failure is approaching.

The analysis is performed on successive, overlapping, time-windows of 512 samples width each, and an overlap of 95 %, i.e. sliding with a step of 26 samples (see Fig. 3). The original EM signal is processed beforehand by running difference. As a result, the first difference time series is analyzed. The unsmoothed FIM time pattern presents quasi-spike-like behaviour, due to the signal's abrupt transitions (Telesca et al., 2010). Therefore, the Fisher information time series of Fig. 3 is depicted smoothed, after a running time-average of 10 windows and 25 % overlapping, to provide a clearer picture of Fisher information temporal evolution.

A comparison of Fig. 3a with Fig. 3b shows a clear difference between the information content of the EM background around the station area (epoch I) and the information content of the precursory signal (epoch II and epoch III).

We note that, the Fisher information values in epoch II, i.e. before the emergence of two strong impulsive bursts in the tail of the pre-seismic EM emission (see Fig. 3), are in general lower than those of epoch III, indicating a smaller amount of information that can be extracted from this set of measurements. Moreover, we observe a significant increase of the Fisher information values specifically during the second strong EM burst. We further discuss the information content of the analysed recording in Sect. 3.4.

3.2 The Shannon entropy in its time-dependent fashion

We calculate subsequently the Shannon entropy, associated with successive time-windows and study its evolution with time. The original EM signal is processed beforehand by running difference. The analysis is also performed on successive, overlapping time-windows of 512 samples width each and an overlap of 95 % , and running time-average of 10 windows and 25 % overlapping (Fig. 4), i.e. under the same analysis parameters as for the Fisher information case.

A comparison of Fig. 4a with Fig. 4b shows a clear difference between the Shannon entropy levels of the EM background around the station area (epoch I) and the Shannon entropy levels of the precursory signal (epoch II and epoch III).

We observe a significant decrease of the Shannon entropy values, as we move to the emerged two strong EM bursts, i.e. moving from epoch II to epoch III (Fig. 4), indicating that a higher degree of order can be traced from the measurements corresponding to epoch III. Furthermore, the Shannon entropy is noticeably lower during the second EM burst. We further discuss the entropy levels of the analysed recording in Sect. 3.4.

3.3 The Tsallis entropy in its time-dependent fashion

The results by means of Tsallis entropy depend upon the entropic index q. Although the appropriate choice of the entropic index q is significant, it still remains to be studied (Naudts, 2002). It is expected that, for every specific use, better discrimination will be achieved with appropriate ranges of values of q (Tsallis, 1998; Abe and Okamoto, 2001). Thus, a question arises: what is the precise q value that describes the system under study?

A model for EQ dynamics coming from a non-extensive Tsallis formalism, starting from fundamental principles, has been recently introduced by Sotolongo-Costa and Posadas (2004). This approach leads to an energy distribution function (Gutenberg–Richter type law) for the magnitude distribution of EQs (see Eq. 8) in Ref. (Sotolongo-Costa and Posadas, 2004). Their equation provides an excellent fit to seismicities generated in various large geographic areas usually identified as seismic regions. Silva et al. (2006) have subsequently revised this model considering the current definition of the mean value, i.e. the so-called q-expectation value. They also suggested an energy distribution function, which provides an excellent fit to seismicities, too:

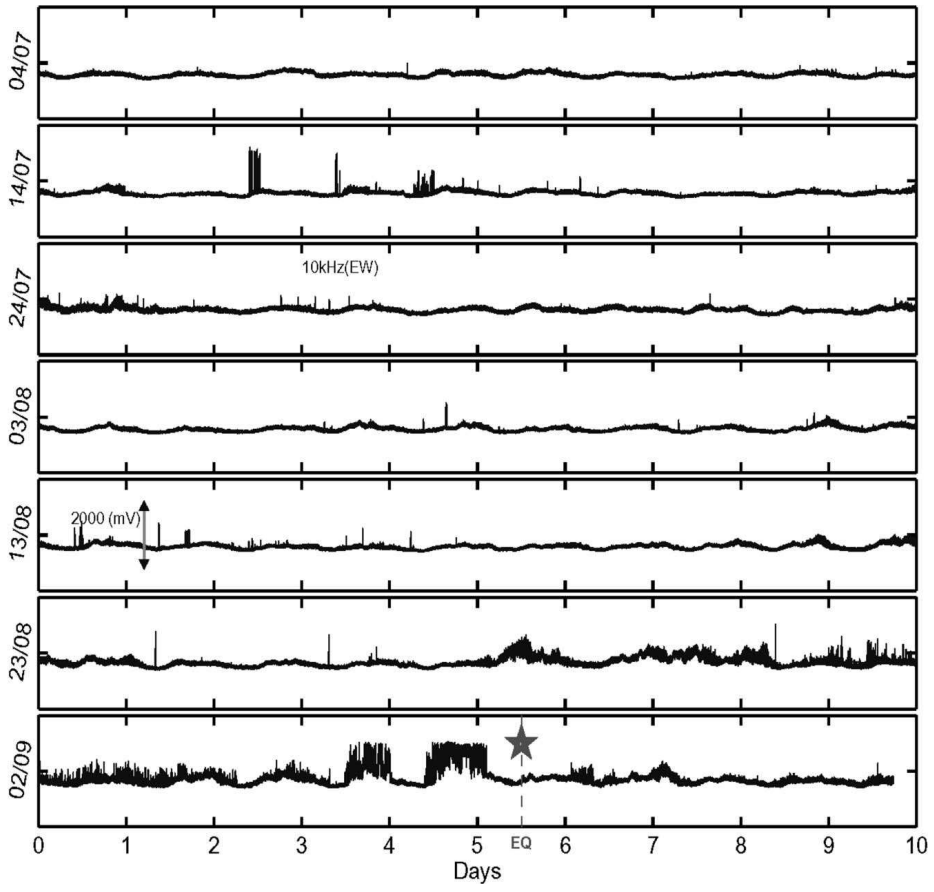

Fig. 1. Time series of the 10 kHz (East-West) magnetic field strength between 4 July and 11 September 1999, in arbitrary units. The star indicates the time of the Athens EQ occurrence. A long duration candidate precursory anomaly emerged from a few days up to a few hours before the EQ. It is clear that the candidate precursor is embedded in a long duration quiescence period concerning the detection of EM disturbances at the kHz frequency band.

$$\log[N(>M)] = \log N + \left(\frac{2-q}{1-q}\right)\log\left[1-\left(\frac{1-q}{2-q}\right)\left(\frac{10^{2M}}{a^{2/3}}\right)\right], \quad (8)$$

where N is the total number of EQs, $N(>M)$ the number of EQs with magnitude larger than M, $M \sim \log\varepsilon$. a is the constant of proportionality between the EQ energy, ε, and the size of fragment, r, $\left(\varepsilon \sim r^3\right)$. Importantly, the associated q-values with the aforementioned Gutenberg–Richter type law (Eq. 8) for different regions (faults) in the world are restricted in the region 1.6–1.7 (Silva et al., 2006) .

Recently, we investigated whether the above-mentioned energy distribution function (Eq. 8), corresponding to non-extensive Tsallis statistics, is able to describe the pre-seismic EM time series. We have shown that Eq. (8) provides an excellent fit to the experimental EM data, incorporating the characteristics of non-extensivity statistics into the distribution of the pre-seismic "electromagnetic EQs" (Papadimitriou et al., 2008) (see also Sect. 4.2.3). The associated q parameter was found to be $q = 1.8$. This finding strongly verifies the sub-extensivity of the underlying fracto-electromagnetic mechanism, while, it is in full agreement with the upper limit $q < 2$ obtained from several studies involving the Tsallis non-extensive framework (Vilar et al., 2007; and references therein). Based on the above mentioned concepts, we estimate the Tsallis entropy for $q = 1.8$.

It is very interesting to observe the similarity in the q values associated with non-extensive Eq. (8) for all the catalogues of EQs used, as well as for the precursory sequences of EM series (Papadimitriou et al., 2008; Eftaxias et al., 2001). The observed similarity in the q values indicates that the activation of a single EQ fault could be considered as a reduced self-affine image of the whole regional seismicity (Papadimitriou et al., 2008; Eftaxias et al., 2001; Kapiris et al., 2003).

Figure 5 shows the Tsallis entropy, associated with successive time-windows and represents its evolution with time. The analysis is once more performed on successive, overlapping, time-windows of 512 samples width each and an

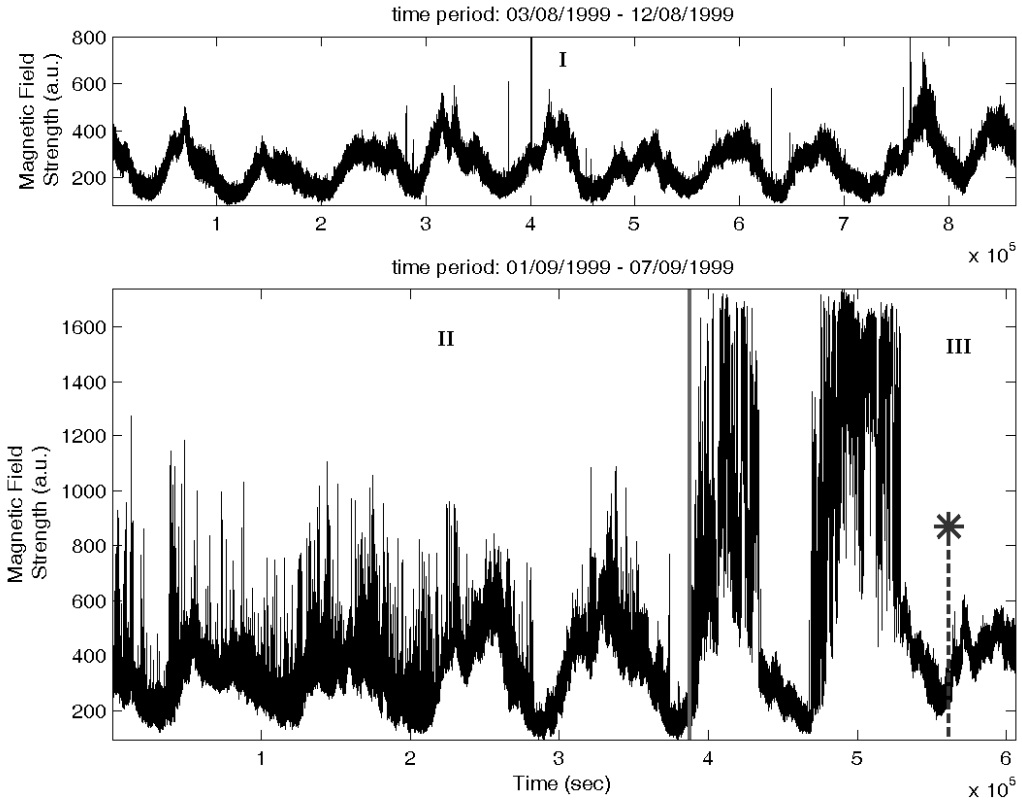

Fig. 2. Focused views of the EM recording. Three different time epochs are noted: the first (I, upper graph) covers from 3 August 1999, 00:00:00 to 12 August 1999, 23:59:59 (UT), the second (II, lower graph) from 1 September 1999, 00:00:00 to 5 September 1999, 11:51:00 (UT), and the third (III, lower graph) from 5 September 1999, 11:51:01 to 7 September 1999, 23:59:59 (UT). A vertical grey line separates epochs II and III. The star indicates the time of the Athens EQ occurrence. The horizontal axis is the time in s, denoting the relative time position from the beginning of each of the focused parts of the EM recording.

overlap of 95 % , and running time-average of 10 windows and 25 % overlapping. The original EM signal is processed beforehand by running difference.

A comparison of Fig. 5a with Fig. 5b shows a clear difference between the Tsallis entropy levels of the EM background around the station area (epoch I) and the Tsallis entropy levels of the precursory signal (epoch II and epoch III).

We observe a significant decrease of the Tsallis entropy values as we move to the emerged two strong EM bursts, i.e. as we pass from epoch II to epoch III. This fact indicates higher organization during epoch III than in epoch II. We also observe that Tsallis entropy is noticeably lower during the second EM burst. We further discuss the entropy levels of the analysed recording in Sect. 3.4.

3.4 Overall considerations

Figure 6 summarizes the temporal evolution of all the employed metrics as the main event is approaching. As mentioned above, in the introduction of this section, three characteristic time periods have been considered, corresponding to three distinctive phases of the EM recording.

The first (3 August 1999, 00:00:00 UT to 12 August 1999, 23:59:59 UT) is far from the EQ occurrence and corresponds to the background noise in the region of the station. Analysing this specific time period of the recording, referred to as epoch I, we define thresholds for the Fisher Information, Shannon entropy, and Tsallis entropy, corresponding to the 95 % limit of the corresponding values distribution. Namely, during this phase, 95 % of Fisher Information values lie below the limit of 1.15, 95 % of Shannon entropy values lie above the limit of 0.73, and 95 % of Tsallis entropy values lie above the limit of 0.885, (Fig. 6a).

Analysing the epochs II and III too (Fig. 6b, and 6c, respectively), we observe a clear differentiation of these two epochs from the background noise. All the used measures indicate an increased order during these two epochs. Furthermore, we can see that the population of "above" threshold values, i.e. above the 1.15 limit for Fisher Information, and below the limits of 0.73 and 0.885 for Shannon entropy and Tsallis entropy, respectively, is significantly higher within the two EM bursts of epoch III, compared to the "above" threshold population of epoch II. Combining these findings with the detailed depiction of the temporal evolution of the

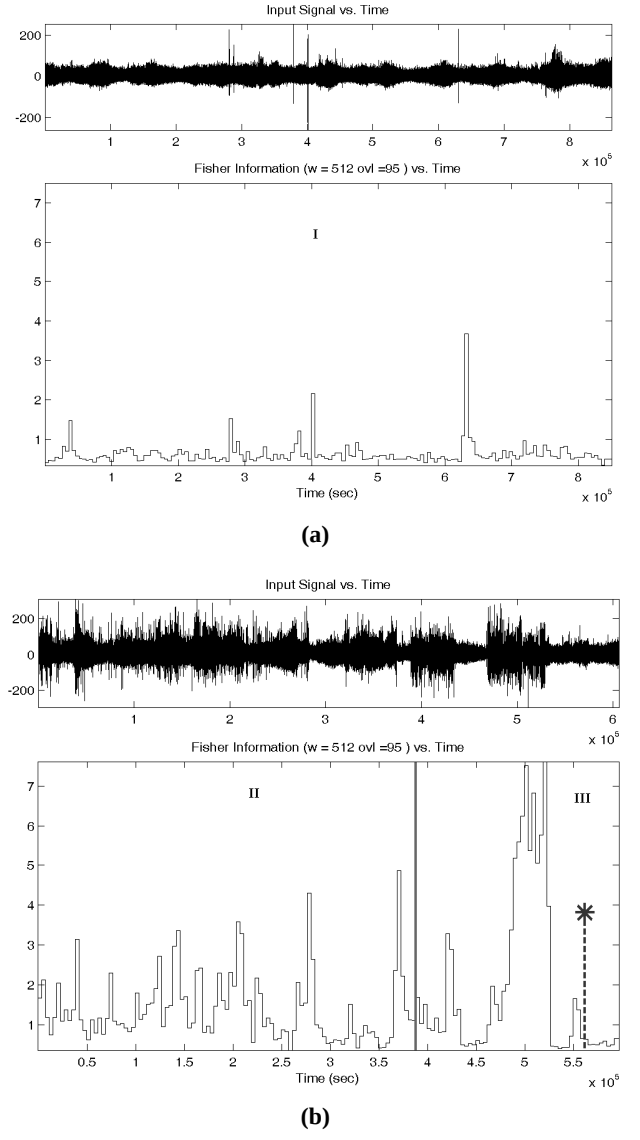

Fig. 3. Fisher information evolution with time **(a)** for epoch I, and **(b)** for the epochs II and III of the signal of Fig. 2. The original EM signal is processed beforehand by running difference. As a result, the first difference time series is analyzed. The analyzed signal is given on top of the resulted Fisher information temporal evolution, time aligned for direct reference. We observe a gradual increase of the Fisher information as the EQ approaches, indicating an increase of the organization of the underlying process.

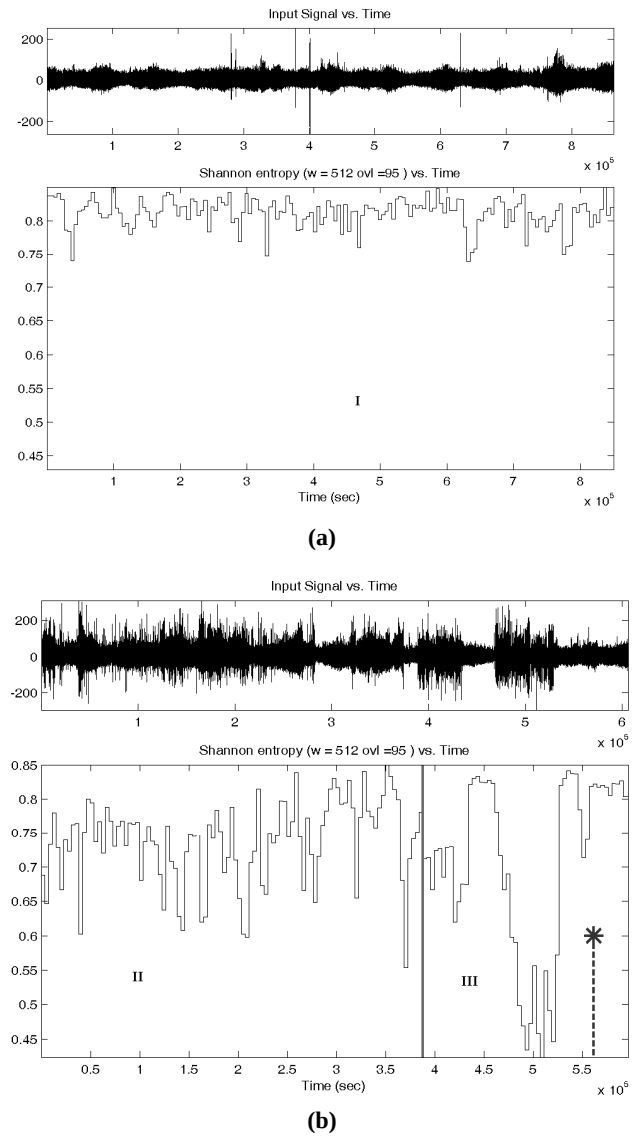

Fig. 4. Shannon entropy evolution with time **(a)** for epoch I, and **(b)** for the epochs II and III of the signal of Fig. 2. The analyzed signal is given on top of the resulted Shannon entropy temporal evolution, time aligned for direct reference. We observe a gradual increase of the organization of the underlying process as the EQ approaches.

used metrics, as presented in Figs. 3, 4, and 5, it is evident that the organized parts of the fracture-induced EM precursor are sparsely distributed in time during epoch II, while on the contrary they are densely distributed in time within the two strong EM bursts of epoch III. This may indicate a qualitative change of the underlying fracto-electromagnetic mechanism. We focus on this point proceeding to spectral fractal analysis for a further investigation.

Previous analyses in terms of spectral fractal analysis have shown that the candidate precursor EM anomaly begins on 1 September 1999, and ends on 7 September 1999 just after the second strong impulsive burst (Kapiris et al., 2004, 2005; Eftaxias et al., 2004). We summarize the results in Fig. 7. More precisely, we have shown that the candidate EM precursor behaves as a temporal fractal; it obeys a power-law of the form:

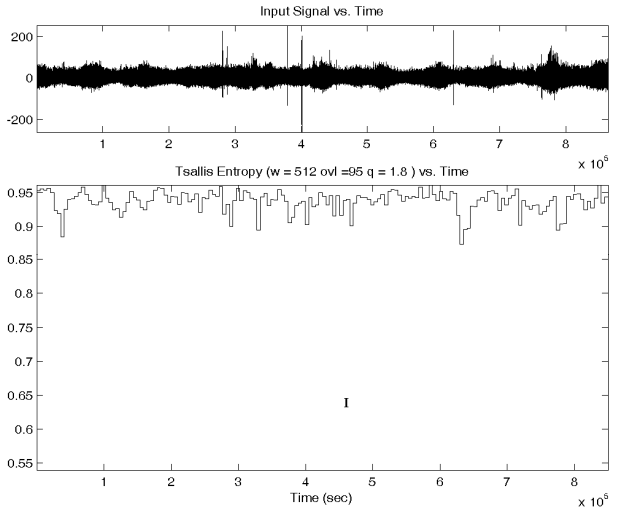

(a)

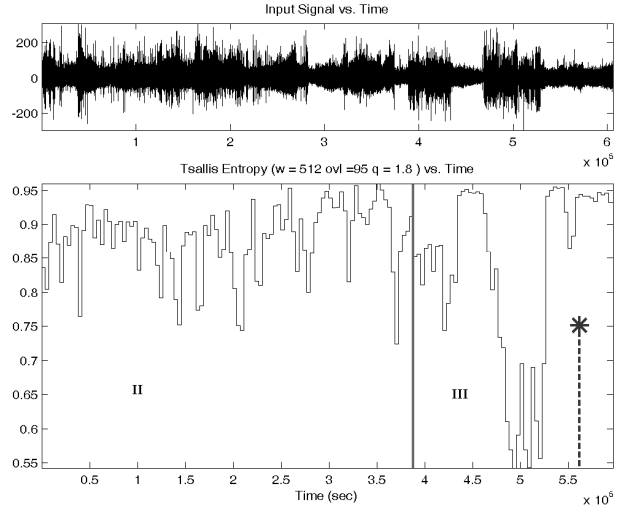

(b)

Fig. 5. Tsallis entropy evolution with time **(a)** for epoch I, and **(b)** for the epochs II and III of the signal of Fig. 2. The analyzed signal is given on top of the resulted Tsallis entropy temporal evolution, time aligned for direct reference. We observe a gradual increase of the organization of the underlying process as the EQ is approaching.

$$S(f) \sim f^{-\beta}, \tag{9}$$

where $S(f)$ is the power spectral density, and f the frequency.

In a $\log S(f) - \log f$ representation the power spectrum is a straight line, with linear spectral slope β. The quality of the fit of a time series to the power-law is represented by the square linear correlation coefficient, r. The temporal evolution of r (see Fig. 7) indicates that the EM time series far from the EQ occurrence (i.e. during epoch I) does not have fractal properties. On the contrary, 58 % of the population of the 1024 samples long consecutive windows included in the first stage of the emerged EM activity (epoch II) fit to the power-law (Eq. 9) with $r > 0.85$. The last rate increases to 99 % into the two strong impulsive EM bursts (the signal part of epoch III), thus the fractal structure is clearly strengthened within the two bursts.

The observed fractal-law indicates the existence of long-term memory. We note that, the larger the β value is, the longer the memory of the underlying mechanism is. Thus, Fig. 7 shows that the memory of the system is increasing as the EQ is approaching. The spectral scaling exponent β, is distributed in the region $1 < \beta < 3$, in the candidate EM precursor.

Two classes of signals have been widely used to model stochastic fractal time series (Heneghan and McDarby, 2000): fractional Gaussian noise (fGn) and fractional Brownian motion (fBm). These are, respectively, generalizations of white Gaussian noise and Brownian motion. For the case of the fGn model the scaling exponent lies between -1 and 1, while the regime of fBm is indicated by values from 1 to 3.

The β-exponent is related to the Hurst exponent, H:

$$\beta = 2H + 1, \tag{10}$$

with $0 < H < 1$ ($1 < \beta < 3$) for the fBm model (Heneghan and McDarby, 2000). The exponent H characterizes the persistent/anti-persistent properties of the signal. The range $0 < H < 0.5$ ($1 < \beta < 2$) indicates anti-persistency, which means that if the fluctuations increase in a time interval, it is likely to decrease in the interval immediately following and vice versa. Physically, this implies that fluctuations tend to induce stability within the system (negative feedback mechanism). Figure 7 reveals that the EM time series exhibits anti-persistent properties during epoch II. On the contrary, the EM precursor exhibits persistent properties, $0.5 < H < 1$ ($2 < \beta < 3$) into the two strong bursts (the signal part of epoch III). This means that if the amplitude of the fluctuations increases in a time interval, it is likely to continue increasing in the immediately next interval. In other words, the underlying dynamics are governed by a positive feedback mechanism.

Analysing the results depicted in Figs. 6 and 7, we suggest the following:

During epoch II

We note an increase of the "above threshold" percentage for all metrics, compared to the background phase (epoch I), signifying an increase of organization in the signal (Fig. 6b). Moreover, the EM activity shows anti-persistent behaviour during this epoch. We note that the population of time-windows having increased anti-persistent organization in respect to that of the background noise is relatively low. We can hypothesize the following physical image. The interplay between the heterogeneities and the stress field could be responsible for the observed pattern. The anti-persistent

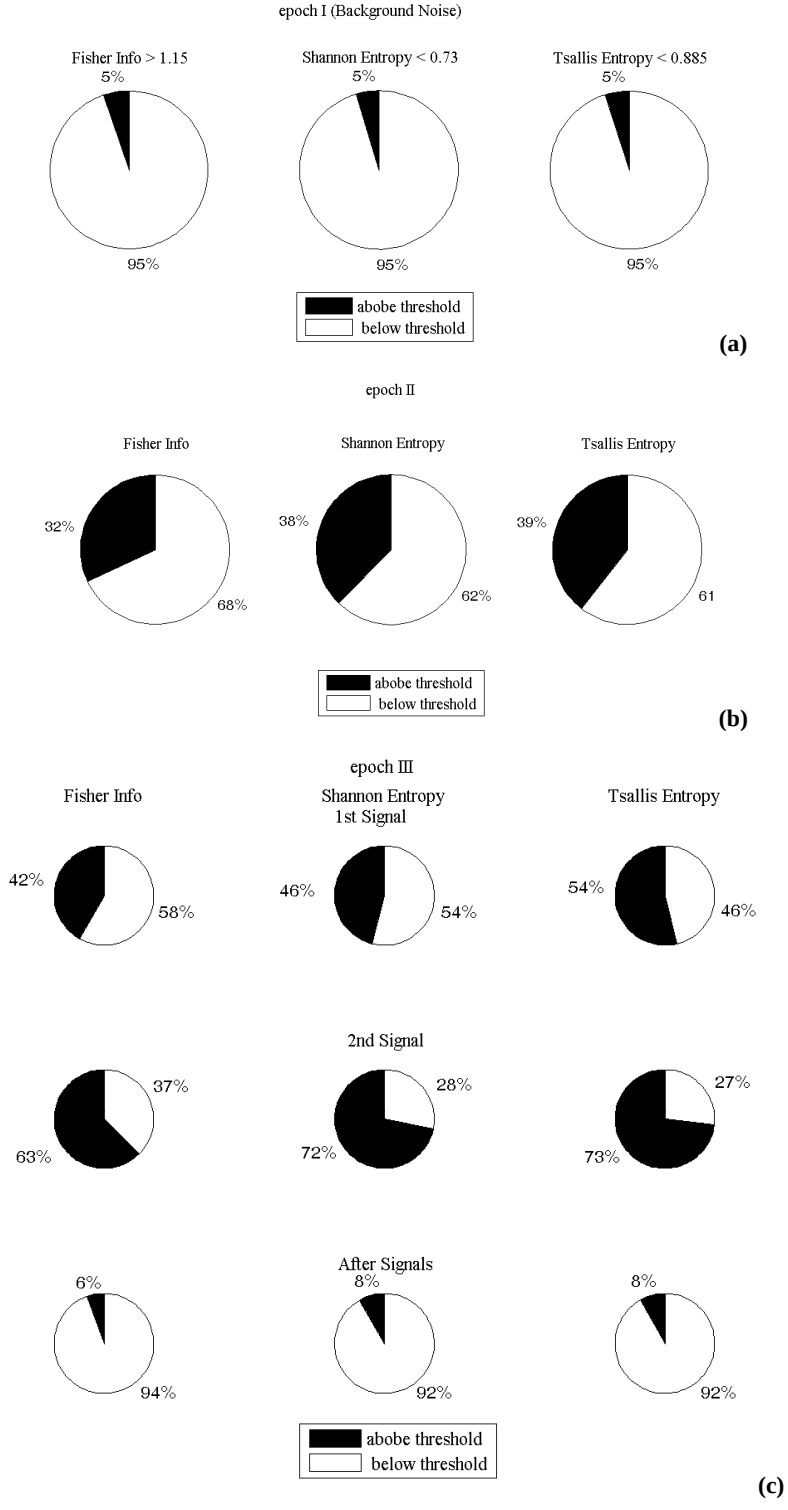

Fig. 6. Percentage of Fisher information, Shannon entropy and Tsallis entropy values lying "above" the background information/entropy threshold. **(a)** Threshold values calculated at the 95 % limit of the information/entropy values distribution during the first, background, phase of the signal (epoch I: 3 August 1999, 00:00:00 UT to 12 August 1999, 23:59:59 UT). "Above threshold" are considered values of Fisher information >1.15, Shannon entropy <0.73, and Tsallis entropy <0.885. **(b)** Percentage of Fisher information, Shannon entropy and Tsallis entropy values "above threshold" for the second, early-preparatory, phase of the signal (epoch II: 1 September 1999, 00:00:00 UT to 4 September 1999, 11:51:00 UT). An increase of the "above threshold" percentage is noted for all metrics, compared to the background percentages, signifying an increased order in the signal. **(c)** The same representation as in **(b)** for the third, main, phase of the signal (epoch III: 5 September 1999, 11:51:01 UT to 7 September 1999, 23:59:59 UT). A further increase of the order is noted inside the two strong signal bursts, while the percentages after the two bursts denote "background" behaviour. It is also pointed out that the second signal appears to be more organized than the first one.

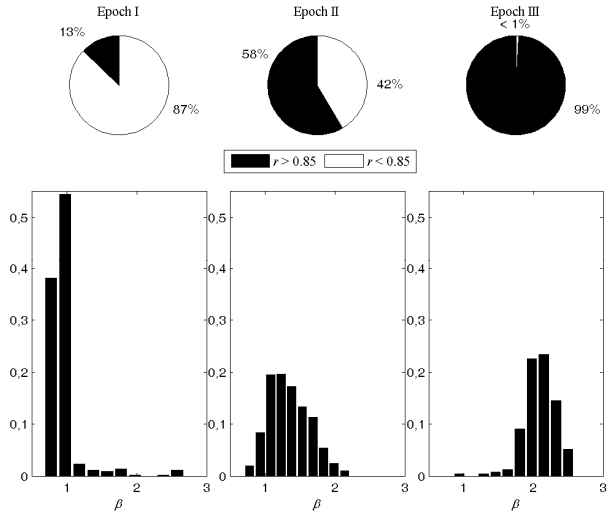

Fig. 7. The lower part shows distribution of the spectral scaling exponent, β, estimated for the population of the short duration windows which presented fitting to power law better than 85 %, over the three epochs of the EM recording under analysis. The upper part shows the percentage of the correlation coefficient, r, lying above the threshold of 0.85 for each one of the three epochs.

character of the EM time series may reflect the fact that in the heterogeneous entities under fracture, entities with a low breaking threshold alternate with much stronger entities. Failure nucleation begins to occur at an area where the resistance to rupture growth has the minimum value. During this fracture, an organized EM emission is emitted. The fracture continues in the same weak area until a stronger area is encountered in its neighbourhood. When this happens, crack growth stops. Then, in the level of EM emission, the EM values come back to the background level. The stresses are redistributed while the applied stress in the focal area increases, thus a new population of cracks nucleates in the weaker of the unbroken areas. The growth of new population of cracks also stops when it encounters another stronger area, and so on. Anti-persistent behaviour implies a set of fluctuations tending to induce stability within the system, i.e. a nonlinear negative feedback, which "kicks" the opening cracks away from extremes.

Epoch III

Epoch III is comprised of two clearly distinguishable parts: the strong impulsive bursts on one hand and the EM recording just after each of them. We observe that outside of the two bursts the "above threshold" percentages indicate "background" behaviour. Regarding the two strong bursts: (i) they are highly organized (Fig. 6c), while the second burst appears to be more organized than the first one. (ii) Both bursts show persistent behaviour. Interestingly, the first burst contains approximately 20 % of the total EM energy received and the second one the remaining 80 % (Eftaxias et al., 2001), see below Sect. 4. (iii) The population of time-windows having high organization is far elevated compared to the organized population of epoch II. The combination of the above mentioned three characteristics leads to the following physical image. The abrupt emergence of strong EM emission in the tail of the precursory EM radiation is regarded as a fingerprint of the local dynamic fracture of nearly homogeneous, high strength, large entities distributed in the focal area sustaining the system. The process is characterized by a positive feedback which leads the system out of equilibrium. Notice that laboratory experiments also show the appearance of high organization and persistency just before the global instability occurrence (Lei et al., 2000; Lei and Satoh, 2007; Ponomarev et al., 1997).

In summary, we argue that the performed statistical analysis by means of Fisher Information, Shannon entropy and Tsallis Entropy reliably distinguishes the candidate EM precursors from the noise: the launch of anomalies from the background state is combined by the appearance of a significantly higher level of organization which increases as the EQ approaches. In the tail the EM activity the appearance of high organization is combined by the emergence of persistency. These two properties are compatible with the last stage of the earthquake preparation process.

4 Interpretation of the EM precursor in terms of seismicity

As it has been proposed in the Introduction, any multidisciplinary statistical analyses by themselves are not sufficient to characterize recorded EM anomalies as pre-earthquake ones. In our opinion, they offer necessary but not sufficient criteria in order to recognize an emergent EM anomaly as a precursor. Both the seismicity and the pre-seismic EM emission represent different cuts in the same underlying fracture mechanism. Thus, we state that if the detected EM anomaly is a result of the EQ preparation process, then, its observed increase of organization as the main event approaches should be an imprint of a corresponding behaviour of the associated seismicity. Therefore, an important pursuit is to make a quantitative comparison between temporal changes of organization hidden in the emergent EM anomaly on one hand, and changes of organization of seismicity on the other hand, as the main event approaches.

Firstly, we attempt to examine in terms of Fisher Information whether the observed organization in the EM precursor under study is also hidden in the seismicity emerged around the epicentre of the Athens EQ prior to the main shock occurrence. Next, we examine the above-mentioned comparison in the frame of a class of models of fracture, which are encompassed by a concept called "Intermittent Criticality" (IC) (Sornette, 2004; Sornette and Sammis, 1995; Saleur et al., 1996a, b; Sammis et al., 1996; Heimpel, 1997). IC bridges

the hypothesis of an underlying self-organized complexity and the occurrence of precursory phenomena (e.g. Huang et al., 1998; Grasso and Sornette, 1998; Hainzl et al., 2000; Newman and Turcotte, 2002; Al-Kindy and Main, 2003).

4.1 Study of seismicity in terms of Fisher Information

We study the seismicity in two geographic areas: (a) within a circle of 200 km radius centred at the Athens EQ epicentre and (b) for the rest of Greece, excluding the area up to 200km around the Athens EQ epicentre. We present these results under the caution that the number of EQs reported from the Institute of Geodynamics of the National Observatory of Athens (http://www.gein.noa.gr/services/cat.html) are limited. Per analysis, parts of equal number of seismic events have been considered for statistical reasons (see Fig. 8). However, first of all we clarify the involvement of the Izmit EQ (Fig. 8) in our study.

The destructive Athens EQ arrived very shortly after the major 17 August 1999, $M_w = 7.4$, EQ of Izmit, Turkey, which occurred approximately 650 km to the NE of Athens. Sufficient seismological measurements suggest a link between the activity in Greece and the Turkish event (Brodsky et al., 2000). Indeed, Brodsky et al. (2000), report that small EQs throughout much of continental Greece followed immediately after the Izmit EQ. The triggering of events in Greece from the Izmit main shock occurred immediately after the passage of the surface waves (Brodsky et al., 2000). Importantly, a time-to-failure analysis showed that the process of small and moderate EQ generation around the epicentre of the Athens EQ (Papadopoulos, 2002) started accelerating immediately after the Izmit EQ the process culminated with a clear short term acceleration similar to the classic foreshock seismicity increase (Papadopoulos, 2002). One hypothesis is that the surface waves of the Izmit EQ might be responsible for the observed positive feedback (Stein, 1999). Notice that, on laboratory scale, Krysac and Maynard (1998) have shown that during the fracture of a brittle material, the breaking of a bond launches a propagating stress wave which may trigger the breaking of other bonds. For this reason we examine the Fisher Information before the time of the Izmit EQ occurrence and after this time up to the time of the Athens EQ occurrence.

The seismicity is examined here in terms of the time intervals between time-neighbouring events from within a given area of interest, namely, within a 200 km radius from the Athens epicentre, and the rest of Greece excluding the area confined by the 200 km radius circle around the Athens EQ epicentre. The seismicity is processed beforehand by running difference. As Fig. 8 shows, the Fisher Information increases right after the occurrence of the Izmit EQ, both outside the 200 km circle around Athens EQ epicentre (Fig. 8b) and inside it (Fig. 8a). This means that the Izmit EQ occurrence is accompanied by the appearance of a significantly higher level of organization in the seismicity of Greece. However,

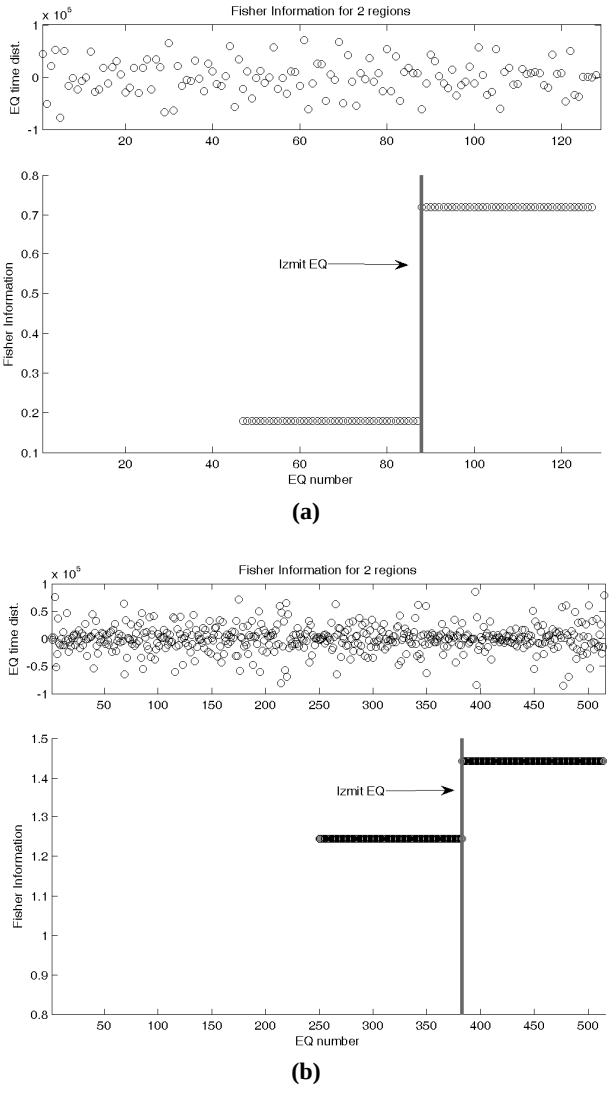

Fig. 8. Fisher information of the seismicity for the EQ events occurring during the time period 20 May 1999 to 7 September 1999, 11:56:50.5 (UT), i.e. up to the time of the Athens EQ occurrence: **(a)** near Athens, i.e. within a 200 km radius from the Athens epicentre, and **(b)** away from Athens, i.e. in the rest of Greece excluding the area confined by the 200 km radius circle around the Athens EQ epicentre. The analyzed time-series is given on top of the resulted Fisher information temporal evolution, time aligned for direct reference. The vertical grey line indicates the time of the Izmit EQ occurrence.

the increase of the Fisher Information which corresponds to the seismicity around the epicentre of the Athens EQ is found to be significantly greater than the increase outside of it. This result supports the hypothesis that the high organization of the detected EM precursor just before the Athens EQ occurrence (Fig. 6) is rooted in the high organization of seismicity around the epicentre of the Athens EQ.

4.2 Interpretation in terms of intermittent criticality

The IC-viewpoint is based on the hypothesis that a large regional earthquake is the end result of a process in which the stress field becomes correlated over increasingly long scale-lengths, which set the size of the largest earthquake that can be expected at any given time. The largest event possible on the fault network cannot occur until regional criticality has been achieved and stress is consequently correlated at all length scales up to the size of the region. This large event destroys, after its occurrence, the criticality on its associated network, creating a period of relative quiescence, after which the process repeats by rebuilding correlation lengths towards criticality and the next large event. In contrast to self-organized criticality, in which the system is always at or near criticality, intermittent criticality implies time-dependent variations in the activity during a seismic cycle.

The central prediction of IC is that large earthquakes only occur when the system is in a critical state. This large EQ acts as a sort of "critical point" dividing the seismic cycle into a period of growing stress correlations before a great earthquake and a relatively uncorrelated stress field after it. Before a large earthquake, the growing correlation length manifests itself as an increase in the frequency of intermediate-magnitude earthquakes. This is commonly referred to as the accelerating moment release model, and has been discussed by a number of authors (Sornette and Sammis, 1995; Sykes and Jaume, 1990; Bufe and Varnes, 1993; Bowman et al., 1998; Jaume and Sykes, 1999; Bowman and King, 2001).

Briefly, the IC approach includes self-organized criticality (Bak and Tang, 1989), growing spatial correlation length (Zöller et al., 2006; and references therein) and accelerating energy release (Bufe and Varnes, 1993; Jaume and Sykes, 1999). We argue that the EM anomaly under study can be interpreted as an EM confirmation of the IC hypothesis.

4.2.1 Focus on the accelerating energy release characteristic

Figure 9 shows the "cumulative EM energy release" $E(t_n) = \sum_{j=1}^{n} E_j, t_n = n \cdot \Delta t, n = 1, 2, 3, \ldots$ (in arbitrary units), where E_j is the released EM energy of the j-th EM event; the EM energy is estimated with the signal energy as defined for a digitized signal $E_j = A_j^2 \cdot \Delta t$, where A_j is the signal amplitude of the j-th EM sample and Δt is the sampling period (here 1 sec). For comparison reasons, we present also, in the same figure, the cumulative seismic energy release computed over a cyclic area ($R = 200$ km) around the epicentre of the Athens EQ, $\varepsilon(t_n) = \sum_{j=1}^{n} \varepsilon_j$, where ε_j is the released energy of the j-th seismic event. The energy release of the j-th seismic event is estimated by the Gutenberg-Richter magnitude-energy relation $\log \varepsilon_j = 1.5 M_j + 11.8$ (Gutenberg, 1956; Kanamori, 1977), where M_j is the magnitude of the j-th seismic event.

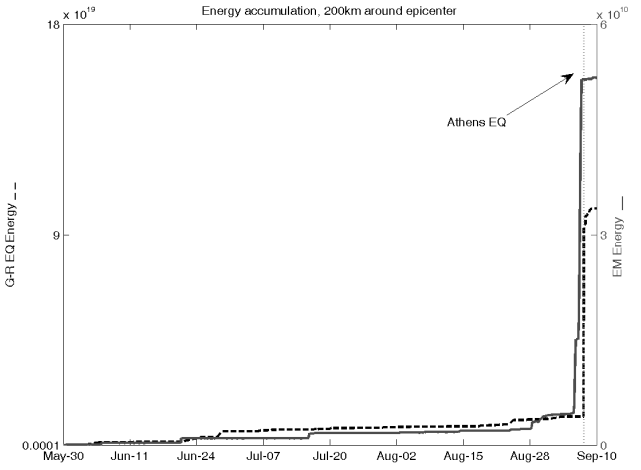

Fig. 9. Time evolution of the EM (continuous line) and seismic (broken line) energy release accumulation. The grey dotted line indicates the time of the Athens EQ occurrence.

One can observe the similarity of the temporal evolution of both the mechanical (seismic) and the EM energy release as the Athens EQ approaches. This experimental fact supports the hypothesis that both the seismicity and the detected pre-seismic EM emission represent two cuts in the same underlying fracture mechanism. It is remarkable that in both cases a power-law type increase in the rate of energy release as the global instability approaches is observed. The observed acceleration of the EM emission leading up to EM large event and "EM shadow" following this could be interpreted as an electromagnetic confirmation of the IC hypothesis.

We pay attention to the subsequent experimental fact. The EM emissions recorded before the Athens EQ end in two very strong bursts (Figs. 1, 2): the first burst contains approximately 20 % of the total EM energy received and the second one the remaining 80 % (Eftaxias et al., 2001). On the other hand, Synthetic Aperture Radars (SAR) are space-borne instruments that emit EM radiation and then record the strength and time delay of the returning signal to produce images of the ground. By combining two or more SAR images of the same area, it is possible to generate elevation maps and surface change maps with unprecedented precision and resolution. This technique is called SAR interferometry. SAR interferometry is becoming a new tool for active tectonics by providing both (i) precision surface change maps spanning periods of days to years and (ii) precision, high-resolution topographic maps for measuring crustal strain accumulated over longer periods of time. Importantly, the fault modelling of the Athens EQ, based on information obtained by radar interferometry (Kontoes et al., 2000), predicts two faults: the main fault segment that is responsible for 80 % of the total energy released, and the secondary fault segment for the

remaining 20 %. Moreover, a seismic data analysis indicates that there was probably a subsequent EQ with magnitude 5.3 after about 3.5 s of the main event (Eftaxias et al., 2001). This experimental result strongly enhances the seismogenic origin of the detected kHz EM emission prior to the Athens EQ.

4.2.2 Focus on the growing spatial correlation length characteristic

Generally, the important feature of spatially extended systems exhibiting a critical behaviour is that the growth of the spatial correlation length obeys a power law with a singularity in the critical point (Bowman et al., 1998; Zöller and Hainzl, 2002; Zöller et al., 2001; Main, 1999). The growing correlation length constitutes an indicator for critical point behaviour prior to large EQs (Zöller et al., 2001; Lee et al., 2009; and references therein).

Maslov et al. (1994) have formally established the relationship between spatial fractal behaviour and long-range temporal correlations for a broad range of critical phenomena. They showed that both the temporal and spatial activity can be described as different cuts in the same underlying fractal. A self-organized critical process, as the source of the temporal power-laws, would further suggest that similar power laws exist also for parameters in the spatial domain (Hansen and Schmittbuhl, 2003). Laboratory experiments also support the consideration that both the temporal and spatial activity can be described as different cuts in the same underlying fractal. Characteristically, Ponomarev et al. (1997) have studied in the laboratory the temporal evolution of Hurst exponent for the series of distances H_r and time intervals H_t between consecutive acoustic emission events in rocks. Their analysis indicates that the changes with time of H_r and H_t are in phase, while the relationship $H_r \sim H_t$ is valid. Based on the above mentioned, a growing correlation length in the EM time series under study could be considered as a footprint of a corresponding growing correlation length of the spatially extended fracture process in the focus area as the main event approaches. Therefore, we examine the existence of a growing correlation length in the EM time series.

We remind the reader here that the EM precursor behaves as temporal fractal obeying the Eq. (9). The spectral scaling exponent β is a measure of the strength of time correlations. We observe that the distribution of the β-exponent is significantly shifted to higher values as the EQ approaches (see Fig. 7). As β increases, the correlation length in the time series also increases. Thus, a basic precursory signature predicted by the IC model is hidden in the candidate EM precursor. The growth of the correlation length in the EM time series under study could be the signature of the growth of the spatial correlation length during the preparation of the impending EQ.

We note that the acceleration in energy release is the consequence of the growth of the spatial correlation length. The long-range correlation without a doubt plays a crucial role to the precursory phenomena in the frame of the IC-approach (Lee et al., 2009). When the long-range correlation happens to the system, it facilitates an initiation of another local fracture in the remote connection and nucleates a new local avalanche which thus averagely increases the avalanche activity (Lahtinen et al., 2005). This situation induces high probability releasing energy to far sites, which furthermore causes a chain of local reactions in toppling around the system (focal area). Thus, the large-scale correlation in the spatial distribution of energy gradually grows, which consequently produces a series of larger and larger events. Therefore, the observed acceleration of the EM energy release and the emission of a series of larger and larger EM events (see Figs. 1, 9) themselves imply a growing correlation length in the EM time series.

4.2.3 Interpretation by means of the long-range connective sandpile model

Lee et al. (2009) have recently analyzed the Hurst exponent H and a power-law exponent B obtained from frequency-size distributions of avalanche events in a long-range connective sandpile (LRCS) model and studied the relation between those two exponents. The LRCS model is introduced by considering the random distant connection between two separated cells. They found that the parameters B and H present precursory phenomena prior to large avalanche events; the B-values typically decrease prior to large avalanches while the H-values increase.

We found that the H-parameter associated with the EM precursor shows the predicted precursory behaviour in terms of H exponent by the LRCS model: H-values increase as the EQ approaches (see Fig. 7).

Concerning the second precursory parameter B, which refers to frequency-size distributions of avalanche events, we study it through the non-extensive Gutenberg-Richter law described by the Eq. (8), which provides an excellent fit to seismicities generated in large geographic areas usually identified as "seismic regions", each of them covering many geological faults.

We refer to the recorded precursory EM time-series $A(t_i)$. We regard as amplitude, $A_{\rm fem}$, of a candidate "fracto-electromagnetic emission" the difference $A_{\rm fem}(t_i) = A(t_i) - A_{\rm noise}$, where $A_{\rm noise}$ is the maximum value of the EM recording during a quiet period, namely far from the time of the EQ occurrence. We consider that a sequence of k successively emerged "fracto-electromagnetic emissions" $A_{\rm fem}(t_i)$, $i = 1, \ldots, k$ represents the EM energy released, ε, during the damage of a fragment. We shall refer to this as an "electromagnetic earthquake" (EM-EQ). Since the squared amplitude of the fracto-electromagnetic emissions is proportional to their energy, the magnitude M of the candidate EM-EQ is given by the relation $M \sim \log\varepsilon = \log\left(\sum [A_{\rm fem}(t_i)]^2\right)$.

Figure 10 shows that Eq. (8) provides an excellent fit to the preseismic EM experimental data, incorporating the

characteristics of non-extensivity statistics into the distribution of the detected precursory EM-EQs. Herein, N is the total number of the detected EM-EQs, $N(>M)$ the number of EM-EQs with magnitude larger than M, $G(>M)=N(>M)/N$ the relative cumulative number of EM-EQs with magnitude larger than M (Sotolongo-Costa and Posadas, 2004; Silva et al., 2006). The best-fit q-parameters for this analysis performed to the EM time series recorded by the 10 kHz EW and 10 kHz NS detectors are given by:

i. 10 kHz EW detector: $q=1.700\pm0.001$ for the second epoch (see Fig. 10a) and $q=1.830\pm0.001$ for the third epoch (see Fig. 10b).

ii. 10 kHz NS detector: $q=1.722\pm0.001$ for the second epoch (see Fig. 10c) and $q=1.8368\pm0.008$ for the third epoch (see Fig. 10d).

It is very interesting to observe the similarity in the q-values of the non-extensive Eq. (8), associated with both the catalogues of the EQs used, and the precursory sequences of EM-EQs under study. The observed similarity in the q-values indicates that the activation of a single EQ (fault) could be considered as a reduced self-affine image of the whole regional seismicity.

The cumulative number of EQs with a magnitude greater than M occurring in a specified area and time is given by the Gutenberg-Richter empirical law:

$$N(>M)\sim 10^{bM}, \tag{11}$$

where b is a constant, which varies only slightly from region to region. The q-parameter included in the non-extensive formula (Eq. 8) is associated with the b parameter by the relation (Sarlis et al., 2010):

$$b=2\cdot\frac{2-q}{q-1} \tag{12}$$

Consequently, the sequence of EM earthquakes are characterized by:

i. 10 kHz EW detector: $b=0.86$ for the second epoch and $b=0.41$ for the third epoch.

ii. 10 kHz NS detector: $b=0.77$ for the second epoch and $b=0.39$ for the third epoch.

We find that the b-values decrease, while the H-values increase in the EM time-series as the EQ approaches, as it is predicted by the long-range connective sandpile model, introduced by Lee et al. (2009).

Based on the above presented analysis, we conclude that the EM anomaly under study actually can be interpreted as an EM confirmation of the IC hypothesis of the EQ generation.

5 Discussion and conclusions

In the present work, we tackle EQs as large scale fracture phenomena. We have attempted to put forward physically meaningful arguments to justify the presence of traces of the last state of earthquake generation within pre-seismic EM emissions. Our method is based on monitoring the fractures which occur in the pre-focal area before the final breakup by recording their kHz–MHz EM emissions.

Tools of information theory (Fisher Information) and concepts of entropy (Shannon and Tsallis entropies) have been used to develop a quantitative identification of kHz EM precursors. We have shown that this analysis reliably distinguishes the candidate EM precursors from the noise: the launch of anomalies from the background state is combined with the appearance of a significantly higher level of organization.

In order to investigate whether the detected EM anomaly is a result of the EQ preparation process, we sought for evidence that its higher level of organization is an imprint of a corresponding higher level of organization of the local seismicity which precedes the EQ occurrence. In this direction, we made a quantitative comparison between the temporal changes of the organization hidden in the emerged EM anomaly on one hand, and the changes of the organization of seismicity on the other hand, as the EQ approaches. We examined the above-mentioned comparison in the frame of a class of models of fracture which are encompassed by a concept called "Intermittent Criticality" (IC). IC-concept bridges the hypothesis of an underlying self-organized complexity to the occurrence of precursory phenomena. We confirmed that the temporal evolution of the detected EM precursor is in harmony with the IC-approach of fracture by means of energy release, correlation length, Hurst exponent, and a power-law exponent obtained from frequency-size distributions of seismic/EM avalanche events.

As it was mentioned in the Introduction, it is reasonable to expect that an EQ's preparatory process has various facets which may be observed before the final catastrophe. Thus, the science of EQ generation/prediction should, from the start, be multi-disciplinary. A candidate EM precursor should be consistent with other precursors that are imposed by data from other disciplines. Thus, a crucial question is whether this necessity is valid for the case presented in this work. The answer is positive. Indeed:

1. We have shown here that the seismological view of the Athens EQ is compatible with the EM one by means of organization (Sect. 4.1), accelerating rate of energy release (Sect. 4.2), IC-hypothesis (Sect. 4.2) and non-extensive model for EQ dynamics (Sect. 4.2).

2. Clear MHz-to-kHz EM anomalies have been systematically detected over periods ranging from a few days to a few hours prior to recent destructive EQs in Greece, with the MHz radiation appearing earlier than the kHz.

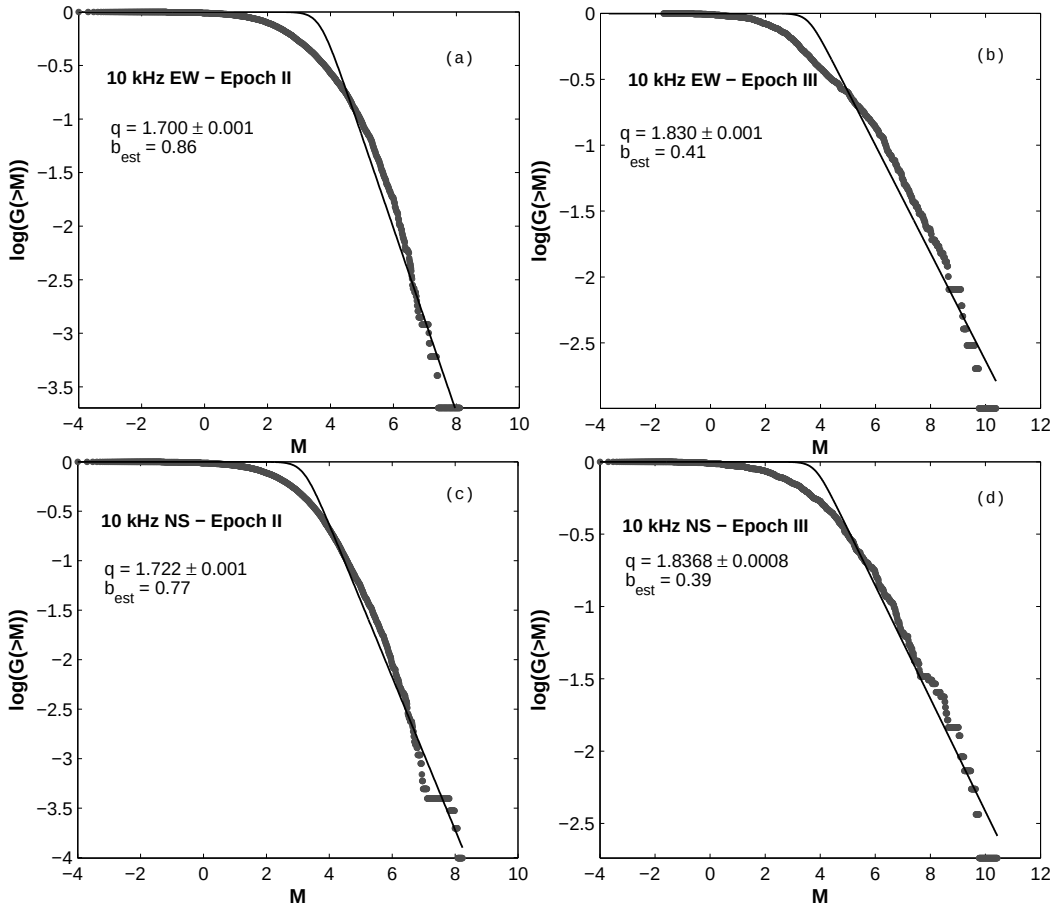

Fig. 10. Equation (8) is used to calculate the relative cumulative number of "electromagnetic earthquakes" (see text), $G(>M)$, included in the epochs II and III defined in Fig. 2, for the EM time-series recorded by the 10 kHz EW (**a** and **b**), and 10 kHz NS detectors (**c** and **d**). A excellent fit of Eq. (8) to the data is observed. The grey dots correspond to the experimental data, while the black curve is the fitting obtained.

A well-documented MHz EM precursor has been detected prior to the Athens EQ (Kapiris et al., 2004; Contoyiannis et al., 2005; Eftaxias et al., 2001, 2007; Contoyiannis and Eftaxias, 2008). The initial MHz anomaly is thought to be due to the fracture of a highly heterogeneous system that surrounds the family of asperities. The associated arguments have been supported by means of criticality, in particular in terms of the recently introduced method of critical fluctuations and Levy statistics (Kapiris et al., 2004; Contoyiannis et al., 2005; Contoyiannis and Eftaxias, 2008).

3. Infrared remote sensing makes use of infrared sensors to detect infrared radiation emitted from the Earth's surface. Enhanced thermal infrared (TIR) emissions from the area of EQ preparation a few days before the seismic shock retrieved by satellites has been frequently reported (Pulinetes and Boyarchuk, 2004; Ouzounov et al., 2005; Tronin et al., 2002; Ouzounov and Freund, 2004). A clear increase in the TIR emission over the area around the Athens EQ epicentre was detected from satellites during the days where the accelerating kHz EM radiation of high organization and persistent behaviour emerged (Filizzola et al., 2004).

4. A type of precursory signals is the so-called seismic electric signals (SES) (Gershenzon and Bambakidis, 2001; Varotsos, 2005). They are ultra-low-frequency (<1 Hz) changes of the electric field of the earth. Field and laboratory experience coincide to the point that the transient low-frequency electric signals SES tend to appear earlier in respect to the MHz-kHz EM emissions. This scheme, namely, the appearance of ultralow frequency changes of the electric field of the Earth followed by kHz-MHz EM precursory radiations, has been reported before the Athens EQs. On 1 and 2 September 1999, a clear SES activity was recorded (Varotsos et al., 1999).

5. We emphasize that the fault modelling of the Athens EQ, based on information obtained by radar interferometry (see Sect. 3.4), predicts two faults: the main fault segment is responsible for 80 % of the total

energy released, and the secondary fault segment for the remaining 20 %. A seismic data analysis also indicates that there was probably a subsequent EQ with magnitude 5.3 after about 3.5 s of the main event (Eftaxias et al., 2001). On the other hand, the first strong EM burst (Figs. 1, 2) contains approximately 20 % of the total EM energy received during the emergence of the two bursts, and the second the remaining 80 % (Eftaxias et al., 2001). This surprising correlation in the energy domain between the two strong pre-seismic kHz EM signals and the two faults activated in the case of the Athens EQ, strongly supports the hypothesis that the two strong EM bursts are sourced in the last stage of the EQ preparation process.

We note that all these various ground and satellite observations led to a converging result: a significant EQ (with magnitude of about 6 or larger) was expected in the area around the Athens in 1999. Even the presented analysis of seismicity in terms of Fisher Information (Sect. 4.1) indicated Athens as the possible position of the epicentre of the finally emerged EQ.

The Earth's crust is clearly extremely complex. However, despite its complexity, there are several universally holding scaling relations. In particular, the aspect of self-affine nature of faulting and fracture is widely documented (Eftaxias et al., 2010; and references therein). Importantly, Huang and Turcotte (1988) have suggested that the statistics of regional seismicity could be merely a macroscopic reflection of the physical processes in the EQ source.

In recent papers, we have shown that the activation of a single fault in terms of pre-seismic kHz EM emissions behaves as a reduced self-affine image of the whole regional seismicity one hand, and a magnified self-affine image of the laboratory seismicity, on the other hand (Papadimitriou et al., 2008; Eftaxias, 2009; Eftaxias et al., 2010). These studies indicate a similarity of the statistical properties of the EM-EQs associated with the activation if a single fault in the energy domain with the laboratory seismicity in terms of acoustic and EM emission on one hand, and seismicity on geological scale on the other hand. The aforementioned similarity has been examined by means of the empirical Gutenberg-Richter law and the Gutenberg-Richter type law rooted in basic principles of non-extensive statistical mechanics.

Under natural conditions it is practically impossible to monitor (much less to control) the principal characteristics of the system under study, namely, the states of stress and strain in the lithosphere and their time variation. Furthermore, it is not possible to repeat experiments under controlled conditions. Thus, the main requirements for a physical experiment are not present. One solution to this problem is to model seismicity in the laboratory by means of acoustic emission (AE) and EM emissions in artificial and natural materials. The basic signatures of laboratory seismicity are hidden in the kHz EM activity under study. Indeed:

1. MHz-to-kHz electromagnetic (EM) anomalies have been detected worldwide over time intervals ranging from a few days to a few hours, while the MHz radiation systematically appears earlier than the kHz (Kapiris et al., 2004; Contoyiannis et al., 2005; Contoyiannis and Eftaxias, 2008; Eftaxias et al., 2002). Laboratory experiments on rock samples reveal a similar change in the frequency content during progressive deformation, i.e. the emissions exhibit a frequency shift from MHz to kHz just before failure of the samples. Pioneering experiments performed by Ohnaka and Mogi (1982) in terms of acoustic emission reveal a significant shift from MHz to kHz just before global failure (97 %–100 % of the failure strength. The aforesaid frequency shift from MHz to kHz has been observed in the case of the Athens EQ .

2. Recent laboratory experiments in terms of both acoustic and EM emission show that the main rupture occurs after the appearance of strong persistent behaviour in the corresponding pre-fracture time-series (Ponomarev et al., 1997; and references therein). This feature is hidden in the EM precursor under study.

3. Laboratory studies under well-controlled conditions i.e. using well-prepared samples containing well-known asperities should be useful for understanding the physics of asperities. Lei et al. (Lei et al., 2000, 2004) have studied how an individual asperity fractures, how coupled asperities fracture, and also the role of asperities in fault nucleation and as potential precursors prior to dynamic rupture. More precisely, the authors suggest the following:

a. Intense microcracking may occur in a strong asperity when the local stress exceeds the fracture stress of the asperity. This feature is in agreement with our results.

b. The self-excitation strength which expresses the influence of excitation of an event on succeeding events or, equivalently, the degree of positive feedback in the dynamics, reaches a maximum during the nucleation phase of the fault. We ask the reader to recall that the Hurst exponent also approaches its maximum value in the tail of the precursory EM radiation under study. These observations reveal a strong similarity between the fracture of asperities in laboratory-scale experiments, individual faults and regional seismicities.

4. Footprints of the universal roughness value of fracture surfaces are hidden in the kHz EM precursor. The Hurst exponent $H \sim 0.7$ has been interpreted as a universal indicator of surface fracture, weakly dependent on the nature of the material and on the failure mode (Hansen and Schmittbuhl, 2003; Gorobei et al., 2005; Mourot et al., 2006; Zapperi et al., 2005). Notice, the surface

roughness of a recently exhumed strike-slip fault plane has been measured. Statistical scaling analyses showed that the striated fault surface exhibits a self-affine scaling invariance that can be described by a scaling roughness exponent, $H = 0.7$ in the direction of slip (Renard et al., 2006). Significantly, the "roughness" of the profile of the kHz EM time series under study is in harmony with the universal roughness value of fracture surfaces.

Although significant problems in extrapolating laboratory results to field conditions remain, the above experimental findings indicate that the emergence of strong positive correlations reflect the faulting nucleation phase of EQ preparation – namely, the fracture of the sequence of asperities in the focal area.

It is a risky practice to extend findings rooted in laboratory experiments to a geophysical scale. However, one cannot ignore the comparison between failure precursors at laboratory and geophysical scales.

It would be desirable to have the possibility to analyze more preseismic EM emissions. However, we stress that in order for it to be possible to extract useful information concerning the preparation of the last stages of the EQ process, the associated EM precursors must satisfy the following requirements. (i) It must have a long duration, that is, from a few tens of hours up to a few days, in order to contain the relevant information. Additionally, a long duration is required in order to use the measurements for statistical purposes. (ii) The recorded radiation must be emerging clearly from the EM background. This means that the detected EM radiation has not been significantly absorbed by conducting layers of the crust or the even more conductive sea, implying that a useful EM precursor must be associated with an on-land seismic event which is both strong, i.e. with magnitude $\sim$6 or greater, and shallow. In this case we have reasons to assert that the fracture process is extended up to the surface layer of the crust, and thus the captured precursory kHz, MHz EM emissions are produced by a population of opening cracks/EM emitters that is sufficient to represent the behaviour of the total number of the activated cracks during the evolution of fracture. However, such strong surface EQs that occur on land are not so common events in a given region such as Greece; the majority of EQs with a magnitude greater or equal to 6 occur in the sea. The potential extension of the performed analysis in regions where strong surface EQs occur on land will offer the possibility for a statistical evaluation of our suggestions in the future.

We emphasize that the complexity of the EQ preparation and the associated pre-seismic EM activities is enormous, and thus, a significant amount of research is needed before we begin to understand it. Whether the presented ideas will prove to be universal will turn out in the future. An extensive amount of combined research is needed before we begin to understand and systematically and accurately predict seismic phenomena. The observed converging results suggest that it is useful to combine various field measurements to enhance the understanding behind the generation of EQs and thus to improve our ability for EQ prediction.

Acknowledgements. The authors would like to thank the reviewers for their constructive comments and suggestions.

Edited by: M. E. Contadakis
Reviewed by: N. Gershenzon and T. Chelidze

References

Abe, S. and Okamoto, Y.: Nonextensive Statistical Mechanics and its Applications, Springer-Verlag, Heidelberg, 2001.

Abe, S., Herrmann, H., Quarati, P., Rapisarda, A., and Tsallis, C.: Complexity metastability, and nonextensivity, in: AIP Conference Proceedings, 95, 2007.

Al-Kindy, F. H. and Main, I. G: Testing self-organized criticality in the crust using entropy: A regionalized study of the CMT global earthquake catalogue, J. Geophys. Res., 108, 2521, doi:10.1029/2002JB002230, 2003.

Bahat, D., Rabinovitch, A., and Frid, V.: Tensile Fracturing in Rocks. Tectonofractographic and Electromagnetic Radiations Methods, Springer, Heidelberg, 2005.

Bak, P. and Tang, C.: Earthquakes as a Self-Organized Critical Phenomenon, J. Geophys. Res., 94, 15635–15637, 1989.

Balasco, M., Lapenna, V., Lovallo, M., Romano, G., Siniscalchi, A., and Telesca, L.: Fisher information measure analysis of earth's apparent resistivity, Int. J. Nonlinear Sci., 5, 230–236, 2008.

Bercher, J.-F.: Some topics on q-gaussians, escort distributions and Fisher information, in 30th International Workshop on Bayesian Inference and Maximun Entropy Methods in Science and Engineering, Chamonix, France, July 4-9, 2010.

Bowman, D., Ouillon, G., Sammis, C., Sornette, A., and Sornette, D.: An observational test of the critical earthquake concept, J. Geophys. Res., 103, 24359–24372, 1998.

Bowman, D. and King, G., J.: Accelerating seismicity and stress accumulation before large earthquakes, Geophys. Res. Lett., 28, 4039–4042, 2001.

Brillouin, L.: The negentropy principle of information, J. Appl. Phys., 24, 1152–1163, 1953.

Brodsky, E., Karakostas, V., and Kanamori, H.: A new observation of dynamically triggered regional seismicity: Earthquakes in Greece following the August 1999 Izmit, Turkey earthquake, Geophys. Res. Lett., 27, 2741–2744, 2000.

Bufe, C. and Varnes, D.: Predictive Modeling of the Seismic Cycle of the Greater San Francisco Bay Region, J. Geophys. Res., 98, 9871–9883, 1993.

Cabezas, H. and Karunanithi, A. T.: Fisher Information, Entropy, and the Second and Third Laws of Thermodynamics, Ind. Eng. Chem. Res., 47, 5243–5249, 2008.

Contoyiannis, Y. F. and Eftaxias, K.: Tsallis and Levy statistics in the preparation of an earthquake, Nonlin. Processes Geophys., 15, 379–388, doi:10.5194/npg-15-379-2008, 2008.

Contoyiannis, Y. F., Kapiris, P. G., and Eftaxias, K. A.: A monitoring of a pre-seismic phase from its electromagnetic precursors, Phys. Rev. E, 71, 066123, 2005.

Cramer, H.: Mathematical Methods of Statistics, Princeton University Press, Princeton, NJ, 1946.

Devroye, L.: A Course on Density Estimation, Birkhauser, Boston, 1987.

Eftaxias, K.: Footprints of nonextensive Tsallis statistics, self-affinity and universality in the preparation of the L'Aquila earthquake hidden in a pre-seismic EM emission, Physica A, 389, 133–140, 2009.

Eftaxias, K., Kapiris, P., Polygiannakis, J., Bogris, N., Kopanas, J., Antonopoulos, G., Peratzakis, A., and Hadjicontis, V.: Signature of pending earthquake from electromagnetic anomalies, Geophys. Res. Lett., 28, 3321–3324, 2001.

Eftaxias, K., Kapiris, P., Dologlou, E., Kopanas, J., Bogris, N., Antonopoulos, G., Peratzakis, A., and Hadjicontis, V: EM anomalies before the Kozani earthquake: A study of their behavior through laboratory experiments, Geophys. Res. Lett., 29, 69/1–69/4, 2002.

Eftaxias, K., Frangos, P., Kapiris, P., Polygiannakis, J., Kopanas, J., Peratzakis, A., Skountzos, P., and Jaggard, D.: Review and a model of pre-seismic electromagnetic emissions in terms of fractal electrodynamics, Fractals, 12, 243–273, 2004.

Eftaxias, K., Panin, V. E., and Deryugin, Y. Y.: Evolution-EM signals before earthquakes in terms of mesomechanics and complexity, Tectonophysics, 431, 273–300, 2007.

Eftaxias, K., Athanasopoulou, L., Balasis, G., Kalimeri, M., Nikolopoulos, S., Contoyiannis, Y., Kopanas, J., Antonopoulos, G., and Nomicos, C.: Unfolding the procedure of characterizing recorded ultra low frequency, kHZ and MHz electromagetic anomalies prior to the L'Aquila earthquake as preseismic ones – Part 1, Nat. Hazards Earth Syst. Sci., 9, 1953–1971, doi:10.5194/nhess-9-1953-2009, 2009.

Eftaxias, K., Balasis, G., Contoyiannis, Y., Papadimitriou, C., Kalimeri, M., Athanasopoulou, L., Nikolopoulos, S., Kopanas, J., Antonopoulos, G., and Nomicos, C.: Unfolding the procedure of characterizing recorded ultra low frequency, kHZ and MHz electromagnetic anomalies prior to the L'Aquila earthquake as pre-seismic ones – Part 2, Nat. Hazards Earth Syst. Sci., 10, 275–294, doi:10.5194/nhess-10-275-2010, 2010.

Epanechnikov, V. A.: Non-parametric estimation of a multivariate probability density, Theory. Probab. Appl., 14, 153–158, 1969.

Fath, R. D., and Cabezas, H.: Exergy and Fisher Information as ecological indices, Ecol. Modelling, 174, 25–35, 2004.

Filizzola, C., Pergola, N., Pietrapertosa, C., and Tramutoli, V.: Robust satellite techniques for seismically active areas monitoring: A sensitivity analysis on September 7th 1999 Athens's earthquake, Phys. Chem. Earth, Part B, 29, 517–527, 2004.

Fisher, R. A.: Theory of statistical estimation, Math. Proc. of the Camb. Phil. Soc., 22, 700–725, 1925.

Frieden, B. R.: Fisher information, disorder, and the equilibrium distributions of physics, Phys. Rev. A, 41, 4265–4276, 1990.

Frieden, B. R.: Physics from Fisher Information. Cambridge University Press, Cambridge, UK, 1998.

Frieden, B. R.: Science from Fisher Information: A Unification. Cambridge University Press, Cambridge, UK, 2004.

Frieden, B. R. and Gatenby, R. A.: Exploratory Data Analysis Using Fisher Information. Springer-Verlag London Limited, 2007.

Frieden, B. R. and Soffer, B. H.: A critical comparison of three information-based approaches to physics, Found. Phys. Lett., 13, 89–96, 2000.

Gershenzon, N. and Bambakidis, G., Modeling of seismo-electromagnetic phenomena, Russ. J. Earth Sci., 3, 247–275, 2001.

Gokhberg, M., Morgounov, V., and Pokhotelov, O.: Earthquake Prediction Seismo-Electromagnetic Phenomena, Gordon and Breach, Singapore, 1995.

Gorobei, N., Luk'yanenko, A., and Chmel, A.: Self-Similar Evolution of the Surface Morphology of a Stressed Amorphous Alloy Foil, J. Exp. Theor. Phys., 101, 468–471, 2005.

Grasso, J.-R. and Sornette, D.: Testing self-organized criticality by induced seismicity, J. Geophys. Res., 103, 29965–29987, 1998.

Gutenberg, B.: The energy of earthquakes, Quart. J. Geol. Soc. London, 112, 1–14, 1956.

Hainzl, S., Zöller, G., and Kurths, J.: Seismic quiescence as an indicator for large earthquakes in a system of self-organized criticality, Geophys. Res. Lett., 27, 597–600, 2000.

Hansen, A. and Schmittbuhl, J.: Origin of the Universal Roughness Exponent of Brittle Fracture Surfaces:Stress-Weighted Percolation in the Damage Zone, Phys. Rev. Lett., 90, 045504, doi:10.1103/PhysRevLett.90.045504, 2003.

Hayakawa, M. and Molchanov, O.: Seismo Electromagnetics, Terrapub, Tokyo, 2002.

Heimpel, M.: Critical behaviour and the evolution of fault strength during earthquake cycles, Nature, 388, 865–868, 1997.

Heneghan, C. and McDarby, G.: Establishing the relation between detrended fluctuation analysis and power spectral density analysis for stochastic processes, Phys. Rev. E, 62, 6103–6110, 2000.

Huang, J. and Turcotte, D.: Fractal distributions of tress and strength and variations of b value, Earth Planet. Sc. Lett., 91, 223–230, 1988.

Huang, Y., Saleur, H., Sammis, C., and Sornette, D.: Precursors, aftershocks, criticality and self-organized criticality, Europhys. Lett., 41, 43–48, 1998.

Humeau, A., Trzepizur, W., Rousseau, D., Chapeau-Blondeau, F., and Abraham, P.: Fisher information and Shannon entropy for on-line detection of transient signal high-values in laser Doppler flowmetry signals of healthy subjects, Phys. Med. Biol., 53, 5061–5076, 2008.

Janicki, A. and Weron, A.: Simulation and Chaotic Behavior of Stable Stochastic Processes, Marcel Dekker, New York, 1994.

Jaume, S. C. and Sykes, L. R.: Evolving towards a critical point: a review of accelerating seismic moment/energy release prior to large and great earthquakes, Pure Appl. Geophys., 155, 279–305, 1999.

Kalimeri, M., Papadimitriou, C., Balasis, G., and Eftaxias, K.: Dynamical complexity detection in pre-seismic emissions using nonadditive Tsallis entropy, Physica A, 387, 1161–1172, 2008.

Kanamori, H.: The Energy Release in Great Earthquakes, J. Geophys. Res., 82, 2981–2987, 1977.

Kapiris, P. G., Eftaxias, K. A., Nomikos, K. D., Polygiannakis, J., Dologlou, E., Balasis, G. T., Bogris, N. G., Peratzakis, A. S., and Hadjicontis, V. E.: Evolving towards a critical point: A possible electromagnetic way in which the critical regime is reached as the rupture approaches, Nonlin. Processes Geophys., 10, 511–524, doi:10.5194/npg-10-511-2003, 2003.

Kapiris, P. G., Eftaxias, K. A., and Chelidze, T. L.: Electromagnetic signature of prefracture criticality in heterogeneous media, Phys. Rev. Lett., 92, 065702, doi:10.1103/PhysRevLett.92.065702, 2004.

Kapiris, P., Polygiannakis, J., Li, X., Yao, X., and Eftaxias, K.: Similarities in precursory features in seismic shocks and epileptic

seizures, Europhys. Lett., 69, 657–663, 2005.

Karamanos, K., Peratzakis, A., Kapiris, P., Nikolopoulos, S., Kopanas, J., and Eftaxias, K.: Extracting preseismic electromagnetic signatures in terms of symbolic dynamics, Nonlin. Processes Geophys., 12, 835–848, doi:10.5194/npg-12-835-2005, 2005.

Karamanos, K., Dakopoulos, D., Aloupis, K., Peratzakis, A., Athanasopoulou, L., Nikolopoulos, S., Kapiris, P., and Eftaxias K.: Study of pre-seismic electromagnetic signals in terms of complexity, Phys. Rev. E, 74, 016104, doi:10.1103/PhysRevE.74.016104, 2006.

Kontoes, C., Elias, P., Sykioti, O., Briole, P., Remy, D., Sachpazi, M., Veis, G., and Kotsis, I.: Displacement field and fault model for the September 7, 1999 Athens earthquake inferred from ERS2 satellite radar interferometry, Geoph. Res. Lett., 27, 3989–3992, 2000.

Krysac, L. C. and Maynard, J. D.: Evidence for the Role of Propagating Stress Waves during Fracture, Phys. Rev. Lett., 81, 4428–4431, 1998.

Lahtinen, J., Kertész, J., and Kaski, K.: Sandpiles on Watts–Strogatz type small-worlds, Physica A, 349, 535–547, 2005.

Lee, Y-T., Chen, C-C., Hasumi, T., and Hsu, H-L.: Precursory phenomena associated with large avalanches in the long-range connective sandpile model II: An implication to the relation between the b-value and the Hurst exponent in seismicity, Geophys. Res. Lett., 36, L02308, doi:10.1029/2008GL036548, 2009.

Lei, X. L., Nishizawa, O., Kusunose, K., Cho, A., Satoh, T., and Nishizawa, O.: Compressive failure of mudstone samples containing quartz veins using rapid AE monitoring: the role of asperities, Tectonophysics, 328, 329–340, 2000.

Lei, X.-L., Masuda, K., Nishizawa, O., Jouniaux, L., Liu, L., Ma, W., Satoh, T., and Kusunose, K.: Detailed analysis of acoustic emission activity during catastrophic fracture of faults in rocks, J. Struct. Geol., 26, 247–258, 2004.

Lei, X. L., and Satoh, T.: Indicators of critical point behavior prior to rock failure inferred from pre-failure damage, Tectonophysics, 431, 97–111, 2007.

Lovallo, M., Marchese, F., Pergola, N., and Telesca, L.: Fisher information analysis of volcano-related advanced, very-high-resolution radiometer (AVHRR) thermal products time series, Physica A, 384, 529–534, 2007.

Main, I.: Applicability of time-to-failure analysis to accelerated strain before earthquakes and volcanic eruptions, Geophys. J. Int., 139, F1–F6, 1999.

Martin, M. T., Pennini, F., Plastino, A.: Fisher's information and the analysis of complex signals, Phys. Lett. A, 256, 173–180, 1999.

Martin, M. T., Pereza, J., and Plastino, A.: Fisher information and nonlinear dynamics, Physica A, 291, 523–532, 2001.

Maslov, S., Paczuski, M., and Bak, P.: Avalanches and 1/f noise in evolution and growth models, Phys. Rev. Lett., 73, 2162, 1994.

Mayer, A. L., Pawlowski, C. W., Cabezas, H.: Fisher Information and dynamic regime changes in ecological systems, Ecol. Modelling, 195, 72–82, 2006.

Mercik, S., Weron, K., and Siwy, Z.: Statistical analysis of ionic current fluctuations in membrane channels, Phys. Rev. E, 60, 7343–7348, 1999.

Mourot, G., Morel, S., Bouchaud, E., and Valentin, G.: Scaling properties of mortar fracture surfaces, Int. J. Fracture, 140, 39–54, 2006.

Naudts, J.: Deformed exponentials and logarithms in generalized thermostatistics, Physica A, 316, 323–334, 2002.

Newman, W. I. and Turcotte, D. L.: A simple model for the earthquake cycle combining self-organized complexity with critical point behavior, Nonlin. Processes Geophys., 9, 453–461, doi:10.5194/npg-9-453-2002, 2002.

Ohnaka, M. and Mogi, K.: Frequency characteristics of acoustic emission in rocks under uniaxial compression and its relation to the fracturing process to failure, J. Geophys. Res., 87, 3873–3884, 1982.

Ouzounov, D. and Freund, F.: Mid-infrared emission prior to strong earthquakes analyzed by remote sensing data, Adv. Space Res., 33, 268–273, 2004.

Ouzounov, D., Pulinets, S., Bryant, N., Taylor, P., and Freund, F.: Satellite thermal infrared radiation before major earthquakes, Geophys. Res. Abstr., 7, 05974, available at: http://www.cosis.net/abstracts/EGU05/05974/EGU05-J-05974-1.pdf, 2005.

Papadimitriou, C., Kalimeri, M., and Eftaxias, K.: Nonextensivity and universality in the EQ preparation process, Phys. Rev. E, 77, 036101, doi:10.1103/PhysRevE.77.036101, 2008.

Papadopoulos, G.: The Athens, Greece, Earthquake (Ms5.9) of 7 September 1999: An Event Triggered by the Izmit, Turkey, 17 August 1999 Earthquake?, B. Seismol. Soc. Am., 92, 312–321, 2002.

Pennini, F., Plastino, A. R., and Plastino, A.: Rènyi entropies and Fisher informations as measures of nonextensivity in a Tsallis setting, Physica A, 258, 446–457, 1998.

Pennini, F., Ferri, G., and Plastino, A.: Fisher Information and semiclassical treatments, Entropy, 11, 972–992, 2009.

Plastino, A., Plastino, A. R., and Miller, H. G.: Tsallis nonextensive thermostatistics and Fisher's information measure, Physica A, 235, 577–588, 1997.

Ponomarev, A., Zavyalov, A., Smirnov, V., and Lockner, D.: Physical modeling of the formation and evolution of seismically active fault zones, Tectonophysics, 277, 57–81, 1997.

Pulinetes, S. A. and Boyarchuk, K.: Ionospheric Precursors of Earthquakes, Springer, Heidelberg, 2004.

Rabinovitch, A., Frid, V., and Bahat, D.: Gutenberg-Richter-type relation for laboratory fracture-induced electromagnetic radiation, Phys. Rev. E, 65, 011401, doi:10.1103/PhysRevE.65.011401, 2001.

Raykar, V. C. and Duraiswami, R.: Fast optimal bandwidth selection for kernel density estimation, in Proceedings of the Sixth SIAM International Conference on Data Mining, Bethesda 2006, 524–528, April 2006.

Renard, F., Voisin, C., Marsan, D., and Schmittbuhl, J.: High resolution 3D laser scanner measurements of a strike-slip fault quantify its morphological anisotropy at all scales, Geophys. Res. Lett., 33, L04305, doi:10.1029/2005GL025038, 2006.

Rundle, J., Turcotte, D., Shcherbakov, R., Klein, W., and Sammis, C.: Statistical physics approach to understanding the multiscale dynamics of earthquake fault systems, Rev. Geophys., 41, 5-15-30, 2003.

Saleur, H., Sammis, C., and Sornette, D.: Discrete scale invariance, complex fractal dimensions, and log-periodic fluctuations in seismicity, J. Geophys. Res., 101, 17661–17677, 1996a.

Saleur, H., Sammis, C. G., and Sornette, D.: Renormalization group theory of earthquakes, Nonlin. Processes Geophys., 3, 102–109, doi:10.5194/npg-3-102-1996, 1996b.

Sammis, C., Sornette, D., and Saleur, H.: Complexity and earthquake forecasting, in Reduction and Predictability of Natural Disasters, in: SFI studies in the Sciences of complexity, edited by: by Rundle, J., Klein, W., and Turcotte, D., Addison-Wesley, Reading, Mass., 1996, XXV, 143–156, 1996.

Sarlis, N. V., Skordas, E. S., and Varotsos, P. A.: Nonextensivity and natural time: The case of seismicity, Phys. Rev. E, 82, 021110, doi:10.1103/PhysRevE.82.021110, 2010.

Shanmugam, S.: Digital And Analog Communication Systems, Wiley India Pvt. Ltd., 2009.

Shannon, C. E.: A Mathematical theory of communication, Bell System Technical Journal, 27, 379–423, 623–656, July, October, 1948.

Silva, R., Franca, G. S., Vilar, C. S., and Alcaniz, J. S.: Nonextensive models for earthquakes, Phys. Rev. E, 73, 026102, doi:10.1103/PhysRevE.73.026102, 2006.

Sornette, D.: Critical phenomena in natural sciences, in: Chaos, Fractals, Self-Organization and Disorder, (2nd ed.), Springer, Heidelberg, 2004.

Sornette, D. and Sammis, C.: Complex critical exponents from renormalization group theory of earthquakes : Implications for earthquake predictions, J. Phys. I. France, 5, 607–619, 1995.

Sotolongo-Costa, O. and Posadas, A.: Fragment-asperity interaction model for earthquakes, Phys. Rev. Lett., 92, 048501, doi:10.1103/PhysRevLett.92.048501, 2004.

Stein, R.: The role of stress transfer in earthquake occurrence, Nature, 402, 605–609, 1999.

Sykes, L. R. and Jaume, S.: Seismic activity on neighbouring faults as a long-term precursor to large earthquakes in the San Francisco Bay area, Nature, 348, 595–599, 1990.

Telesca, L., Lapenna, V., and Lovallo, M.: Fisher Information Analysis of earthquake-related geoelectrical signals, Nat. Hazards Earth Syst. Sci., 5, 561–564, doi:10.5194/nhess-5-561-2005, 2005a.

Telesca, L., Lapenna, V., and Lovallo, M.: Fisher information measure of geoelectrical signals, Physica A, 351, 637–644, 2005b.

Telesca, L., Caggiano, R., Lapenna, V., Lovallo, M., Trippetta, S., and Macchiato, M.: The Fisher information measure and Shannon entropy for particulate matter measurements, Physica A, 387, 4387–4392, 2008.

Telesca, L., Lovallo, M., Ramirez-Rojas, A., and Angulo-Brown, F.: A nonlinear strategy to reveal seismic precursory signatures in earthquake-related selfpotential signals, Physica A, 388, 2036–2040, 2009.

Telesca, L., Lovallo, M., and Carniel, R.: Time-dependent Fisher Information Measure of volcanic tremor before the 5 April 2003 paroxysm at Stromboli volcano, J. Volcan. Geoth. Res., 195, 78–82, 2010.

Telesca, L., Lovallo, M., Hsuc, H.-L., and Chenc, C.-C.: Analysis of dynamics in magnetotelluric data by using the Fisher–Shannon method, Physica A, 390, 1350–1355, 2011.

Tronin, A., Hayakawa, M., and Molchanov, O.: Thermal IR satellite data application for earthquake research in Japan and China, J. Geodyn., 33, 519, 2002.

Tsallis, C.: Possible generalization of Boltzmann_Gibbs statistics, J. Stat. Phys., 52, 479–487, 1988.

Tsallis, C.: Generalized entropy-based criterion for consistent testing, Phys. Rev. E, 58, 1442–1445, 1998.

Tsallis, C.: Introduction to Nonextensive Statistical Mechanics, Approaching a Complex Word. Springer, New York, 2009.

Uyeda, S., Nagao, T., and Kamogawa, M.: Short-term EQ prediction: Current status of seismo-electromagnetics, Tectonophysics, 470, 205–213, 2009.

Varotsos, P.: The Physics of Seismic Electric Signals, Terrapub, Tokyo, 2005.

Varotsos, P., Eftaxias, K., Hadjicontis, V., Bogris, N., Skordas, E., Kapiris, P., and Lazaridou, M.: A note on the extent of the SES sensitive area around Lamia (LAM), Greece, Acta Geophys. Polonica, 47, 435–444, 1999.

Vignat, C. and Bercher, J.-F.: Analysis of signals in the Fisher–Shannon information plane, Phys. Lett. A, 312, 27–33, 2003.

Vilar, C., Franca, G., Silva, R., and Alcaniz, J.: Nonextensivity in geological faults?, Physica A, 377, 285–290, 2007.

Zapperi, S., Nukala, P., and Simunovic, S.: Crack roughness and avalanche precursors in the random fuse model, Phys. Rev. E, 71, 026106, doi:10.1103/PhysRevE.71.026106, 2005.

Zöller, G. and Hainzl, S.: A systematic spatiotemporal test of the critical point hypothesis for large earthquakes, Geophys. Res. Lett., 29, 53/1–53/4, doi:10.1029/2002GL014856, 2002.

Zöller, G., Hainzl, S., and Kurths, J.: Observation of growing correlation length as an indicator for critical point behavior prior to large earthquakes, J. Geophys. Res., 106(B2), 2167–2175, 2001.

Zöller, G., Hainzl, S., Ben-Zion, Y., and Holschneider, M.: Earthquake activity related to seismic cycles in a model for a heterogeneous strike-slip fault, Tectonophys., 423, 137–145, 2006.

Zunino, L. , Perez, D., Kowalski, A., Martin, M., Garavaglia, M., Plastino, A., and Rosso, O.: Fractional Brownian motion, fractional Gaussian noise, and Tsallis permutation entropy, Physica A, 387, 6057–6088, 2008.